의학박사 학위논문

Neurotoxic action of oxidized TRPC5 in abnormal glutathione homeostasis

S-glutathionylation of TRPC5

by GSSG as a novel activator

TRPC5 이온통로의 S-glutathionylation에 의한 신경독성 효과

2013년 08월

서울대학교 대학원

의과학과 의과학 전공

홍 찬 식

A thesis of the Degree of Doctor of Philosophy

TRPC5 이온통로의 S-glutathionylation 에 의한 신경독성 효과

Neurotoxic action of oxidized TRPC5 in abnormal glutathione homeostasis

S-glutathionylation of TRPC5 by GSSG as a novel activator

August 2013

The Department of Biomedical Sciences

Seoul National University

College of Medicine

Chansik Hong

Neurotoxic action of oxidized TRPC5 in abnormal glutathione homeostasis

S-glutathionylation of TRPC5 by GSSG as a novel activator

by

Chansik Hong

A thesis submitted to the Department of Biomedical science in partial fulfillment of the requirements for the Degree of Doctor of Philosophy in Medical Science (Biomedical Science) at Seoul National University College of Medicine

July 2013

Approved by Thesis Committee:

Professor _____(Chairman)
Professor _____(Vice chairman)
Professor _____
Professor _____
Professor _____

TRPC5 이온통로의 S-glutathionylation에 의한 신경독성 효과

지도 교수 서 인 석

이 논문을 의학박사 학위논문으로 제출함

2013년 04월

서울대학교 대학원

의과학과 의과학 전공

홍 찬 식

홍찬식의 의학박사 학위논문을 인준함

2013년 07월

위 원 장 _____ (인)

부위원장 _____ (인)

위 원 _____ (인)

위 원 _____ (인)

위 원 _____ (인)

ABSTRACT

Introduction : The pathogenesis of neurodegenerative disorders is induced by aberrant neuronal calcium (Ca^{2+}) signaling, while normal Ca^{2+} in neuron occurs as a result of the physiologic process. Recent studies indicate that TRPC, a member of the TRP subfamily of Ca^{2+}-permeant, non-selective cation channel, plays an important role in mediating cellular responses to a wide range of stimuli such as oxidants that can induce intracellular Ca^{2+} dysregulation under certain situations. However, the molecular basis of TRPC channel involvement in these processes is not fully understood.

Results : Here, I measured that several oxidants, DTNP (125 ± 25 pA/pF, *n*=6), DTNB (12 ± 3 pA/pF, *n*=6), 2-PDS (122 ± 58 pA/pF, *n*=6) and H_2O_2 (47 ± 19 pA/pF, *n*=6), activate TRPC5 or TRPC4 currents by recording in whole cell configuration. Depending on intracellular levels of glutathione, oxidized glutathione (GSSG) as well as oxidizing agents affected the activity of TRPC4/C5. Also I suggested that C176 and C178 of cytosolic conserved cysteines in TRPC4/C5 are directly modified by oxidants, and particularly glutathionylated by GSSG using co-Immunoprecipitation (Co-IP) assay for S-glutathionylated protein detection. Using clonal striatal cell lines from wild-type (ST*Hdh*$^{Q7/7}$) and mutant huntingtin knock-in (ST*Hdh*$^{Q111/111}$) mice, I identified that TRPC4 and TRPC5 are endogenously expressed in the cell line. The change of intracellular glutathione level (e.g. GSH/GSSG ratio, depleted GSH) by incubation with carmustine (BCNU) or L-buthionine (S,R) sulfoximine (BSO) induced cell death in HD cell line. In the effect of BCNU or BSO, ST*Hdh*$^{Q111/111}$ was more sensitive than ST*Hdh*$^{Q7/7}$. After pretreatment with BSO, H_2O_2 at lower concentration is susceptible to reduction in the cell density of both cell lines. When applied FRET-based Ca^{2+} imaging, cytosolic Ca^{2+} remained as a persistent state of high level with preincubated BCNU. Transient transfection with small interfering RNA (siRNA) of TRPC5 or the pretreatment with a blocker of TRPC channel, 10 μM cadmium chloride ($CdCl_2$) or 10 μM ML204 significantly attenuated BCNU-induced cell death using flow cytometry or MTT assay.

Conclusions : I clarify the role of TRPC5 in Huntington's disease, showing the neuronal apoptosis that caused by abnormal cytosolic Ca^{2+} through TRPC5, and demonstrate a route of calcium via activation mechanism suggested that cytosolic GSSG oxidizes to protein S-glutationylation (PSSG) in TRPC5.

Keywords: TRPC5, oxidant, glutathione, Huntington's disease
Student number: 2009-21910

CONTENTS

LIST OF FIGURES AND TABLES

Figure

Table

LIST OF ABBREVIATIONS

TRPC : Canonical or transient receptor potential ion channel

DTNP : 2,2 -dithiobis(5-nitropyridine) / 5-nitro-2-PDS

DTNB : 5,5 -dithiobis(2-nitrobenzoic acid)

2-PDS : 2,2 -dithiodipyridine

DTT : Dithiothreitol

TCEP : Tris(2-carboxyethyl)phosphine

GSH : Reduced glutathione

GSSG : Oxidized glutathione, Glutathione disulfide

BCNU : 1,3-bis(2-chloroethyl)-N-nitrosourea, Carmustine

BSO : L-buthionine (S,R)sulfoximine

INTRODUCTION

Neurodegenerative diseases (NDs) comprise an increasing proportion of the debilitating illnesses that confront an aged society globally. Age-related degenerative diseases include Alzheimer's disease (AD), Parkinson's disease (PD), Huntington's disease (HD), amyotrophic lateral sclerosis (ALS, also known as Lou Gehrig's disease) and Friedreich's ataxia (FRDA) that are characterized by progressive loss of neurons in the central or peripheral nervous system. These diseases have been implicated in neuronal cell death by protein misfolding, excitotoxicity, activation of cell death pathways, mitochondrial dysfunction, increased iron deposition and oxidative stress through the excessive reactive oxygen species (ROS) and/or reactive nitrogen species (RNS) (1). Although oxidation reactions are critical for life, they can also be highly toxic and rapidly detoxified; plants and animals maintain multiple (nonenzymatic and enzymatic) types of complex antioxidant systems. Under insufficient levels of antioxidants, or inhibition of the antioxidant enzymes, the generation of

reactive oxygen species (ROS) and oxidative damage in neuronal cells can aggravate neurodegenerative disorders. The brain is particularly vulnerable to oxidative stress due to high energy needs (high oxygen consumption), paucity of antioxidants compared to other organs, and large lipid content (2).

Among various antioxidant systems including vitamin as well as enzymes such as catalase, superoxide dismutase and various peroxidases, glutathione (GSH) is a ubiquitous non-protein thiol-containing molecule found at millimolar concentrations in eukaryotic cells. It is a tripeptide composed of cysteine, glutamic acid, and glycine and its active group contains the sulfur (SH) chemical groups of cysteine residue as a reducing power. It maintains high level in the cell and plays essential physiological functions in DNA and protein synthesis, transport and redox reaction, such as free radical scavenging and cellular detoxification. In cells, GSH is mainly present in its reduced form, which can be converted to the oxidized form during oxidative stress, and can be reverted to the reduced form by GSH reductase. The ratio of GSH to glutathione disulfide (GSSG) contributes to the redox potential of the cell and thereby to

redox homeostasis (3). Oxidative stress leads to a decreased GSH/GSSG ratio and formation of mixed disulfide bonds between GSH or GSSG and redox-sensitive cysteine residues within proteins (4,5).

Protein reactive cysteines can be involved in modulation of its protein activity via modification of their thiol (sulfhydryl; -SH), interacting with GSH or GSSG (S-glutathionylation or Protein-SSG). In addition, the post-translational modifications at free cysteines can take several forms, such as protein disulfide, S-nitrosylation or S-glutathionylation. Recent studies show cysteine-based oxidation is involved in gene expression, cell death or survival (6), energy metabolism, protein folding and degradation (7), etc. These cellular responses are mediated by signaling proteins or ion channels such as NMDA (8), RyR (9), calcium or potassium channel and TRP channel; TRPA1 (10), TRPM2 (11) through methione (Met214) oxidation.

Transient receptor potential channels (TRP channels), ubiquitously expressed in numerous human and animal cell types, mediate a variety of sensations like pain, hotness, warmth, coldness, tastes, vision, and pressure such as osmotic

pressure, volume, stretch, and vibration, as well as redox state. Among 6 TRP-family channels, the seven mammalian canonical or classical transient receptor potential (TRPC) channels are divided into four subgroups, TRPC1, TRPC2, TRPC3/6/7 and TRPC4/5, based on sequence similarities. TRPC1, TRPC4 and TRPC5 are close homologs, sharing 64% identity with many cysteine residues. TRPC5 is a Ca^{2+}-permeable cationic channel that modulates properties of mammalian cells including neurons and endothelial cells (12,13). It can form channels on its own or assembled with other related proteins such as TRPC1 and TRPC4. Each channel is thought to require four TRPC proteins to assemble around a central ion pore. The channels show constitutive activity and voltage dependence but they are also stimulated by a range of factors including agonists at G protein-coupled receptors, lysophospholipids, acidification, and redox factors. And it has been suggested that the channels are stimulated by nitric oxide (NO) through a mechanism that requires direct S-nitrosylation of TRPC5 at two extracellular cysteine residues (C553 and C558) near the ion pore (14). However, the conclusions are difficult to reconcile with data, suggesting that breaking a disulphide bridge at same cysteine

residues activates TRPC channels (15,16).

Here I thought conserved cysteines of TRPC4/C5 are dynamically relevant to GSH/GSSG ratio in redox reaction. It has been reported that oxidative stress leads to degenerative neurological diseases under certain condition such as GSH depletion, dysregulation of GSH/GSSG and reduced antioxidant activity (17). On this basis, I confirmed if unexpected TRPC5 oxidation induced abnormal calcium signaling, resulting in Huntington's disease (HD). Taken together, I hypothesized that TRPC channels contribute to oxidative stress-induced and Ca^{2+}-dependent neuronal cell damage via cysteine-based oxidation depending on intracellular redox status, especially glutathione. My results open new prospects for neurodegenerative disorders via new mechanism of TRPC4/C5 by glutathione.

MATERIALS AND METHODS

Cell culture, Transient transfection, and cDNA plasmids

Human embryonic kidney (HEK)-293 cells were purchased from American Type Culture Collection (ATCC, U.S.A.). Clonal striatal cell lines from wild-type (ST*Hdh*$^{Q7/7}$) or mutant huntingtin knock-in (ST*Hdh*$^{Q111/111}$) mice were from Dr. H. Ryu (18). The cells were maintained in Dulbecco's modified Eagle's medium (Hyclone, U.S.A.), supplemented with 10% fetal bovine serum, 100 U/ml penicillin, and 100 μg/mL streptomycin according to the supplier's recommendations. The cells were seeded in 6 or 12-well plates in accordance with each experiment. Plasmids containing human TRPC5 (hTRPC5) or mouse TRPC5 (mTRPC5) were kindly donated by Dr. S. Kaneko or Dr. Y. Mori (14), respectively. For multiple cysteine mutation, single mutants of mTRPC5, received from Mori, were changed to serine on the desired cysteine sites in an overlapped manner using QuickChange site-directed mutagenesis (Agilent Technologies, U.S.A.). For transient transfection, the vector containing the GFP-tagged cDNA of hTRPC5 or mTRPC5 transfected into HEK cells cultured to 60-

80% confluence using FuGENE 6 transfection reagent (Roche Molecular Biochemicals, Germany) according to the manufacturer's protocol. All experiments were performed after 20-30h from transfection.

Chemicals and antibodies

All chemicals (DTNB, 2-PDS, DTT, GSH, GSSG, BSO, H_2O_2, BCNU, NAC) were purchased from Sigma Aldrich (U.S.A.) except TCEP from Thermo Scientific (U.S.A.).

Electrophysiology

Transfected cells in 12-well plate were trypsinized and transferred into a recording chamber equipped to treat with a number of solutions. Whole cell currents were recorded using an Axopatch 200B amplifier (Axon Instruments, U.S.A.). Currents were filtered at 5 kHz (-3 dB, 4-pole Bessel), digitized using a Digidata 1440A Interface (Axon Instruments), and analyzed using a personal computer equipped with pClamp 10.2 software (Axon Instruments) and Origin software (Microcal origin v.8.0, U.S.A.). Patch pipettes were made from borosilicate glass and had resistances of 2-4 MΩ when filled with standard intracellular solutions. For whole cell

experiments, I used the standard pipette solution contained (in mM) 140 CsCl, 10 *N*-[2-hydroxyethyl]piperazine-*N*' -[2-ethanesulfonic acid] (HEPES), 0.2 Tris-GTP, 0.5 EGTA, and 3 Mg-ATP with pH adjusted to 7.3 using CsOH. Intracellular 3 mM GSH or various concentration of GSSG pipette solution was included to the standard pipette solution, except in the case of adding GSH or GSSG. The external bath medium (normal Tyrode solution) of the following composition (in mM): 135 NaCl, 5 KCl, 2 $CaCl_2$, 1 $MgCl_2$, 10 glucose, and 10 HEPES with pH adjusted to 7.4 using NaOH. For TRPC4, Cs^+-rich external solution was made by replacing NaCl and KCl with equimolar CsCl. Voltage ramp pulse was applied from +100 to −100 mV for 500 ms at −60 mV holding potential. For TRPC1, voltage ramp pulse was applied from +100 to −120 mV. Calculated junction potential between the pipette and bath solutions used for all cells during sealing was 5 mV (pipette negative) using pClamp 10.2 software. No junction potential correction was applied. Experiments were performed at room temperature (18-22 ℃). Cells were continuously perfused at a rate of 0.5 ml/min. All current traces were drawn from the selected value at −60 or +80 mV of ramp pulse. For all bar graphs, inward current amplitude was summarized at −60 mV.

FRET-based Ca^{2+} measurement using Cameleon YC6.1

3 FRET images (cube settings for CFP, YFP, and Raw FRET) were obtained from a pE-1 Main Unit to 3 FRET cubes (excitation, dichroic mirror, filter) through a fixed collimator: CFP (ET435/20m, ET CFP/YFP/mCherry beamsplitter, ET470/24m, Chroma); YFP (ET500/20m, ET CFP/YFP/mCherry beamsplitter, ET535/30m, Chroma); and Raw FRET (ET435/20m, ET CFP/YFP/mCherry beam-splitter, ET535/30m, Chroma). The excitation LED and filter were sequentially rotated, rotation period for each of filter cubes was ~0.5 s, and all images (three for CFP/YFP/Raw FRET, respectively) were obtained within 1.5 s. Each of the images was captured on a cooled 10 MHz (14 bit) CCD camera (DR-328G-C01-SIL: Clara, ANDOR technology, USA) with an exposure time of 100 ms with 2 × 2 binning (645 × 519 pixels) under the control of MetaMorph 7.6 software (Molecular Devices, Japan). To obtain the FRET efficiency of a cell, I used a microscope (IX70, Olympus, Japan) with a 60× oil objective and the three-cube FRET method calculation (19). Calcium mobilization was measured by using cameleon YC6.1 (generous gift from M. Ikura (20)), an engineered calcium indicator based

on the dependence of CaM conformation on elevations of calcium concentration. An increase in calcium binding to CaM leads to a decrease in the distance separating the two flanking proteins, CFP and YFP, and results in a measurable FRET change. Using a single excitation wavelength at 405 nm, which solely excites CFP, images and fluorescence emissions data for both CFP and YFP were collected. The experiments were performed in live neurons in the absence of extracellular calcium, and the data obtained from each individual cell were used to calculate the ratios, reflective of the energy transferred. The background signal was subtracted from the values obtained after drug injection.

Western blot, Surface biotinylation, and Co-IP

Cells were plated in 6-well dishes. Lysates were prepared in lysis buffer (0.5% Triton X-100, 50 mM Tris-Cl, 150 mM NaCl, 1 mM EDTA, pH 7.5) by passing 7-10 times through a 26-gauge needle after sonication. Lysates were centrifuged at 13,300 g for 10 min at 4 ℃, and protein concentration in the supernatants was determined. The proteins extracted in sample buffer were loaded onto 6 or 8% tris-glycine SDS-PAGE gels.

Gels were transferred onto PVDF membrane, and western blot analysis was done.

For surface biotinylation, PBS-washed cells were incubated in 0.5 mg/ml sulfo-NHS-LC-biotin (Pierce) in PBS for 30 min on ice. Afterwards, the biotin was quenched by the addition of 100 mM glycine in PBS. The cells were then processed as described above to make cell extract. 40 μl of a 1:1 slurry of immobilized avidin beads (Pierce) were added to 300 μl of cell lysates (500 μg protein). After incubation for 1 h at RT, beads were washed three times with 0.5% Triton-X-100 in PBS, and proteins were extracted in sample buffer. Collected proteins were then analyzed by Western blot.

For the Co-IP experiments, 500 μl of cell lysates were incubated with 1 μg of GSH antibody and 25 μl of protein G-agarose beads at 4 ℃ overnight with gentle rotation. Subsequently, the beads were washed three times with wash buffer (0.1% Triton X-100, 50 mM Tris-Cl, 150 mM NaCl, 1 mM EDTA, pH 7.5), and the precipitates were eluted with 30 μl of 2× Laemmli buffer and subjected to Western blot analysis.

MTT cell death assay

Q7 or Q111 cells were grown in 12-well culture plates. MTT

assay was used to assess cell viability according to the manufacturer's instructions (Sigma-Aldrich). The assay was quantitated by measuring the absorbance at 570 nm using a micro-plate spectrophotometer (Biochrom, U.K.).

Flow cytometry analysis (FACS)

After treatment with BCNU, the harvested cells were then placed in fluorescence-activated cell sorter (FACS) buffer (PBS with 0.1% bovine calf serum, 0.05% sodium azide) at 4 ℃ for 30 min. After being washed with FACS buffer, cells were analyzed using a FACSCalibur flow cytometer equipped with Cell Quest software (BD Pharmingen, U.S.A.).

Gene silencing using siRNA (siTRPC1 and siTRPC5)

For gene silencing, the siRNA was transfected using the RNAi Max Transfection Reagent (Invitrogen, U.S.A.), according to the manufacturer's instructions. Mouse TRPC5 siRNA (Cat.1441728) were purchased from Bioneer. Control siRNA was purchased from Dharmacon (Cat.D-001210-01-05). The silencing effects were evaluated using RT-PCR as described in Supplemental information.

Intracellular Ca^{2+} measurement

The ratiometric measurement of $[Ca^{2+}]_i$ was performed using Fura-2-AM (molecular probe). The cells were grown in 24-well dishes and loaded with 5 μM of Fura-2-AM for 30 min at 37 ℃. The Fura-2 fluorescence was measured at a 510 nm emission with a 340/380 nm dual excitation using a DG-4 illuminator. The experiments were performed in a normal Tyrode solution (in mM) containing 145 NaCl, 3.6 KCl, 10 HEPES, 2 $CaCl_2$, 1 $MgCl_2$, and 5 glucose with pH adjusted to 7.4 using NaOH.

Reverse transcription polymerase chain reaction analysis

Total RNA was extracted from Q7 or Q111 cells using TRIzol reagent (Invitrogen). Reverse transcription was performed using a commercial kit according to the manufacturer's instruction (Invitrogen). RT-PCR of mouse TRPC4 and TRPC5 mRNA was performed using TRPC4 forward primer (TCA GCA CAT CGA CAG GTC AGA C), TRPC4 reverse primer (CCA CGG TAA TAT CAT CCA CTC CAC), TRPC5 forward primer (TAG TAC TAC TGG CTT TTG CCA ACG), and TRPC5

reverse primer (ATT CAG CAG CAC TAC CAG GGA GAT). The following conditions were used for PCR: pre-heating (94 ℃, 2 min), 35 cycles of denaturation (94 ℃, 30 sec), annealing (50 ℃, 30 sec), extension (72 ℃, 60 sec), and final extension (72 ℃, 10 min).

Statistics

Results are given as mean ± S.E.M. Results were compared using Student's *t*-test between two groups, or using ANOVA followed by post hoc test among three groups or more. $p < 0.05$ was considered statistically significant. The number of cell electrical recordings is given by *n* in bar graph

RESULTS

Effects of oxidants on TRPC4/C5 current

There are two contradictory suggestions about the activation of TRPC via oxidation (14) or reduction (15) reaction. In their works, this redox reaction activated homomeric TRPC5 or heteromeric TRPC1/C5 based on extracellular cysteines between transmembrane 5 and 6. Although TRPC4 also assembles to form heteromultimeric pore structures with TRPC1 and/or C5 sharing high similarity with them in sequence, structure, and functional property (21), they didn't show or obtain the activation in TRPC4. Accordingly, I asked if not only does any process of redox reaction (oxidation / reduction) regulate TRPC channels but also TRPC4 is mediated.

Here, I treated the several oxidants and reductants which are the same agents used by Yoshida (14) and Xu (15) to reproducibly investigate the effect of redox agents on TRPC4/C5. To efficiently measure TRPC4 activity, I used a Cs^+−rich solution (140 mM Cs^+) on both the intracellular $[Cs^+]_i$ and extracellular sides $[Cs^+]_o$ on the basis of high permeability of Cs^+ ion in TRPC4 (22). TRPC5 but not TRPC4 channels have

a basal activity under normal Tyrode solution (135 mM Na^+). To show the typical doubly-rectifying current (*I*)-voltage (*V*) relation and inward current on TRPC4/C5, I applied ramp pulse from +100 to -100 mV for 500 ms at a holding potential of -60 mV using the whole-cell patch clamp techniques.

As shown in Figure 1 and Figure 2, reactive disulfides acting on free sulfhydryl groups of cysteine residues in proteins activated TRPC4β as well as TRPC5. Membrane-permeable pyridyldisulfides (PDS) such as 2,2 -dithiobis(5-nitropyridine) (DTNP, 125 ± 25 pA/pF, Fig.1A) and 2,2 -dithiodipyridine (2-PDS, 122 ± 58 pA/pF, Fig.1B) induced Na^+ current in cells expressing TRPC5, whereas membrane impermeable analog 5,5 -dithiobis(2-nitrobenzoic acid) (DTNB, 12 ± 3 pA/pF, Fig.1C) activated TRPC5 channels in case of treatment on the intracellular side that was indistinguishable from the treatment on extracellular side (Fig.1D). Hydrogen peroxide (H_2O_2, 47 ± 19 pA/pF, Fig.1E) increased TRPC5 activity. In similar manner, TRPC4β channels were activated by DTNP (42 ± 17 pA/pF, Fig. 2A), 2-PDS (28 ± 12 pA/pF, Fig. 2B) or DTNB (19 ± 5 pA/pF, Fig. 2C) in condition of extracellular Cs^+-rich solution (140 mM Cs^+). In addition to my electrophysiologic approach, I

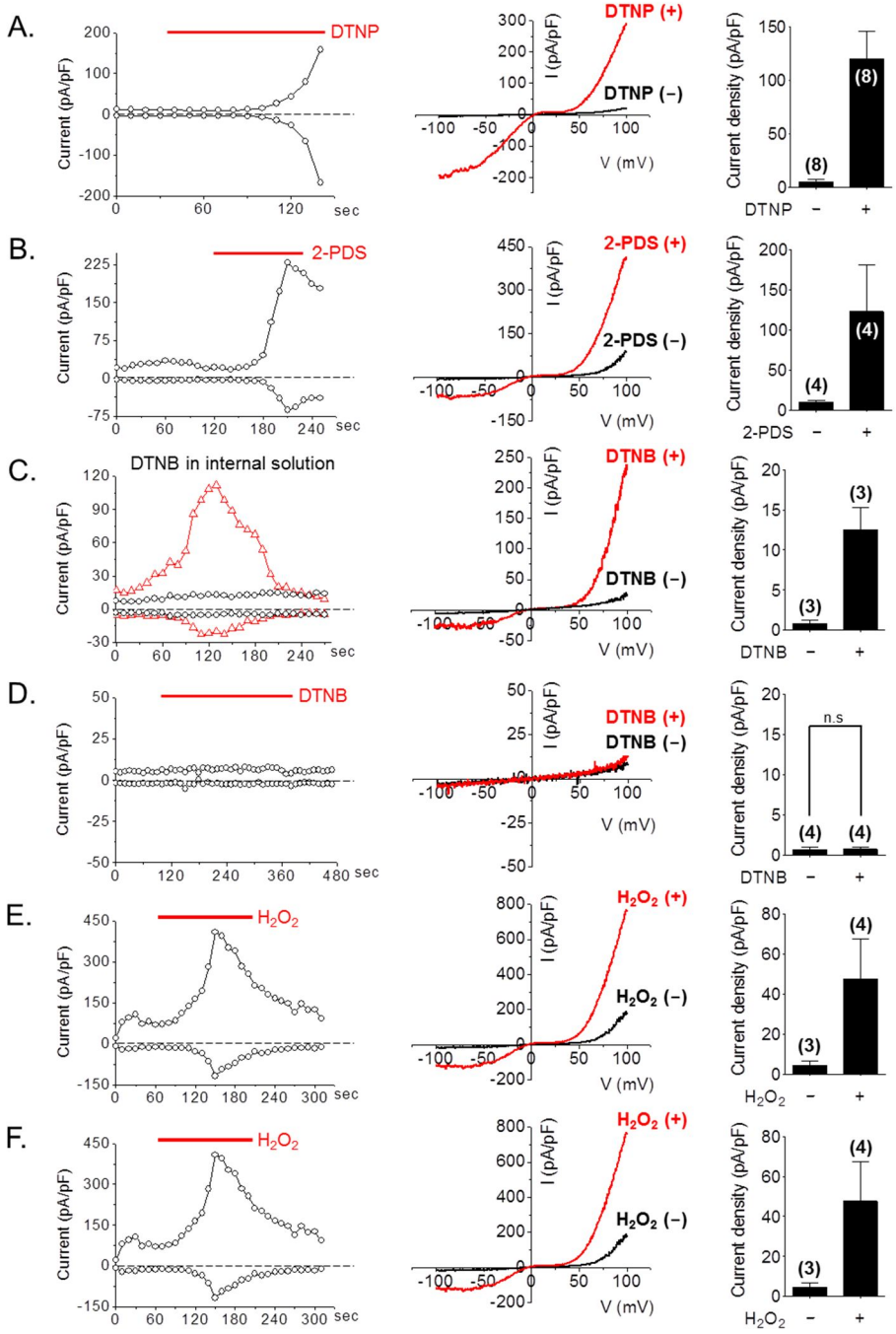

Fig. 1 Effects of oxidants on TRPC5 activity

In hTRPC5-expressing HEK cells, TRPC5 currents were recorded under the condition of normal Tyrode solution. Two colored lines indicate application with the chemical (red) or

without the chemical (black) in current trace or Current (*I*)－Voltage (*V*) relationship. In bar graph, the number indicates the recorded cell numbers (*N*) with patch clamp. Statistics of results is shown as $*P<0.05$ or no significance (n.s).

A. ***Left***, A representative current trace of TRPC5 activated by 30 μM DTNP. ***Middle***, A *I*－*V* curve of a typical doubly rectifying TRPC5 by DTNP. ***Right***, A summarized bar graph of inward current amplitudes of TRPC5 by DTNP at －60 mV.

B. ***Left***, A representative current trace of TRPC5 activated by 100 μM 2－PDS. ***Middle***, A *I*－*V* curve of a typical doubly rectifying TRPC5 by 2－PDS. ***Right***, A summarized bar graph of inward current amplitudes of TRPC5 by 2－PDS at －60 mV.

C. ***Left***, A representative current trace of TRPC5 activated by internally infused 200 μM DTNB. ***Middle***, A *I*－*V* curve of a typical doubly rectifying TRPC5 by DTNB. ***Right***, A summarized bar graph of inward current amplitudes of TRPC5 by DTNB at －60 mV.

D. ***Left***, A representative current trace of TRPC5 by externally treated 1 mM DTNB. ***Middle***, A *I*－*V* curve of a non－activated TRPC5 by DTNB. ***Right***, A summarized bar graph of inward current amplitudes of TRPC5 by DTNB at －60 mV.

E. ***Left***, A representative current trace of TRPC5 activated by 1 mM H_2O_2. ***Middle***, A *I*－*V* curve of a typical doubly rectifying TRPC5 by H_2O_2. ***Right***, A summarized bar graph of inward current amplitudes of TRPC5 by H_2O_2 at －60 mV.

F. ***Left***, A representative trace of intracellular Ca^{2+} response by 1 mM H_2O_2 in hTRPC5－expressing HEK cells through fluorescent $[Ca^{2+}]_i$ measurements technique using the Fura－2. ***Right,*** A summarized fluorescence intensity induced by H_2O_2 at 340 / 380 nm.

measured intracellular Ca^{2+} level via a fluorescent $[Ca^{2+}]_i$ measurement technique using Fura-2 to investigate whether TRPC5 channel activity is accompanied by Ca^{2+} influx as well as monovalent cation, Na^+ or Cs^+. In transfected HEK cells with TRPC5, 30 μM DTNP or 1 mM H_2O_2 also induced transient Ca^{2+} increase (Fig. 1F).

These results imply that oxidants can activate TRPC4β or C5 channels, resulting in the influx of extracellular cations into cytosol. Although I don't show the reduction effect of TRPC4/C5 by reducing agents as Xu et al. (15), my results are similar to intracellular Ca^{2+} experiment investigated by Yoshida et al. (14), except TRPC4β. I noted internal DTNB-induced TRPC4β/C5 activation, unlike external DTNB, and decided to investigate which side (inside or outside of the cell) is mediated in activation of TRPC4β/C5 by oxidants using reductants differing in permeability of the membranes.

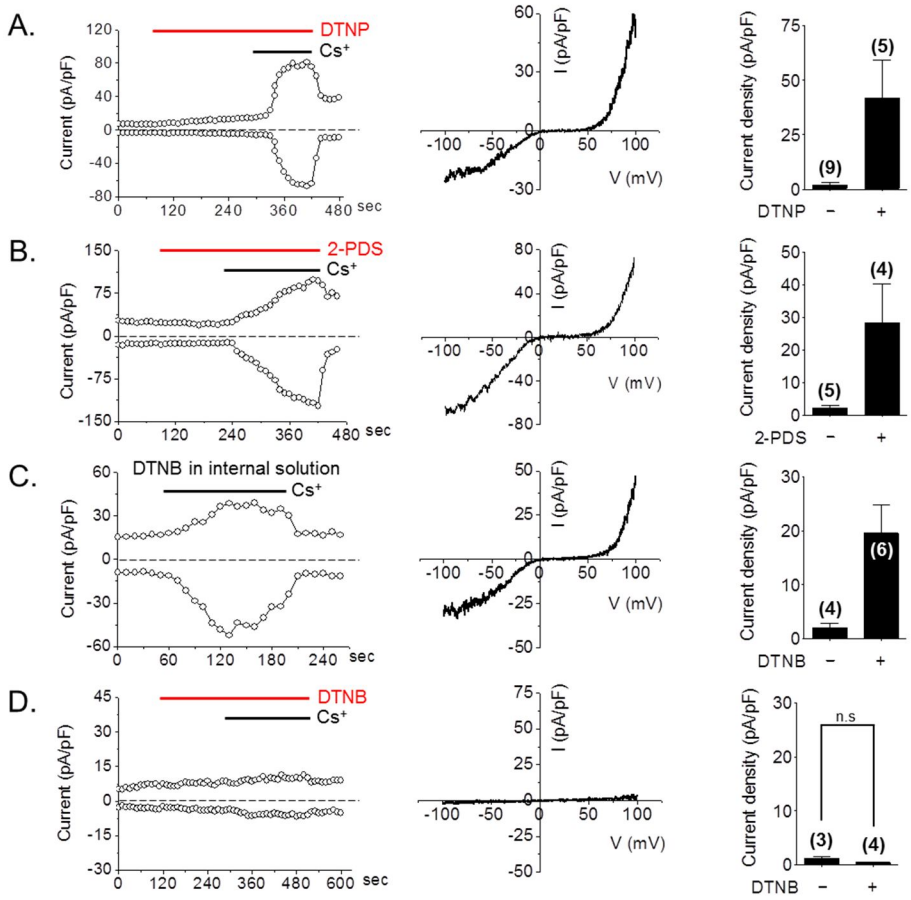

Fig. 2 Effects of oxidants on TRPC4β activity

In mTRPC4β-expressing HEK cells, TRPC4β currents were recorded under the condition of 140 mM $[Cs^+]_o$ solution. Two colored lines indicate application with the chemical (red) or without the chemical (black) in current trace or Current (*I*)-Voltage (*V*) relationship. In bar graph, the number indicates the recorded cell numbers (*N*) with patch clamp. Statistics of results is shown as $*P<0.05$ or no significance (n.s).

A. ***Left***, A representative current trace of TRPC4β activated by 30 μM DTNP. ***Middle***, A *I*-*V* curve of a typical doubly rectifying TRPC4β by DTNP. ***Right***, A summarized bar graph of inward current amplitudes of TRPC4β by DTNP at −60 mV.

B. ***Left***, A representative current trace of TRPC4β activated by 100 μM 2−PDS. ***Middle***, A $I-V$ curve of a typical doubly rectifying TRPC4β by 2−PDS. ***Right***, A summarized bar graph of inward current amplitudes of TRPC4β by 2−PDS at −60 mV.

C. ***Left***, A representative current trace of TRPC4β activated by internally infused 200 μM DTNB. ***Middle***, A $I-V$ curve of a typical doubly rectifying TRPC4β by DTNB. ***Right***, A summarized bar graph of inward current amplitudes of TRPC4β by DTNB at −60 mV.

D. ***Left***, A representative current trace of TRPC4β by externally treated 1 mM DTNB. ***Middle***, A $I-V$ curve of a non−activated TRPC4β by DTNB. ***Right***, A summarized bar graph of inward current amplitudes of TRPC4β by DTNB at −60 mV.

Effects of reductants on oxidant (DTNP)-activated TRPC4/C5 current

I identified which side is mediated in oxidation, returning oxidation effect to the reduced state using two reductants (DTT and TCEP) that have different membrane permeability. Cell permeable DTNP-induced TRPC5 currents were slowly reversed by membrane-permeable DTT to basal activity via chemical reduction (Fig. 3A). However, cell-impermeable TCEP showed that DTNP-activated TRPC5 currents still remain (Fig. 3B). In TRPC4, the activation effect of DTNP was reversible by DTT to the state prior to treatment with DTNP (Fig. 4A). When TCEP, unlike DTT, was treated in bath solution after the activation by DTNP, activated TRPC4β currents was not diminished (Fig. 4B). Interestingly, DTT, but not TCEP, showed additional transient activation (~20 sec) in activated state of TRPC5 (data not shown) and then was returned to basal activity within several seconds (as Fig. 3A). I think the reason of both ways in DTT as follows; The front of transient activation may be caused by Ca^{2+} dependent endoplasmic reticulum (ER) stress induced by DTT (23), because intracellular calcium itself can activate TRPC5 (24). And the next DTT effect can break the oxidation to modified form (S-S-TNP) by DTNP, removing a activating factor of

TRPC5.

These results imply that the oxidants-activated TRPC4β/C5 channels are involved in intracellular oxidative process in cytosol. To rigorously control cellular oxidation, the reducing environment of the cytoplasm is relevant to redox homeostasis and antioxidant signaling. I noted oxidized glutathione (GSSG) and its reduced counterpart, GSH that has been called "the master antioxidant", because GSSG can dysfunction as a potential time-bomb when failed to regulate glutathione homeostasis.

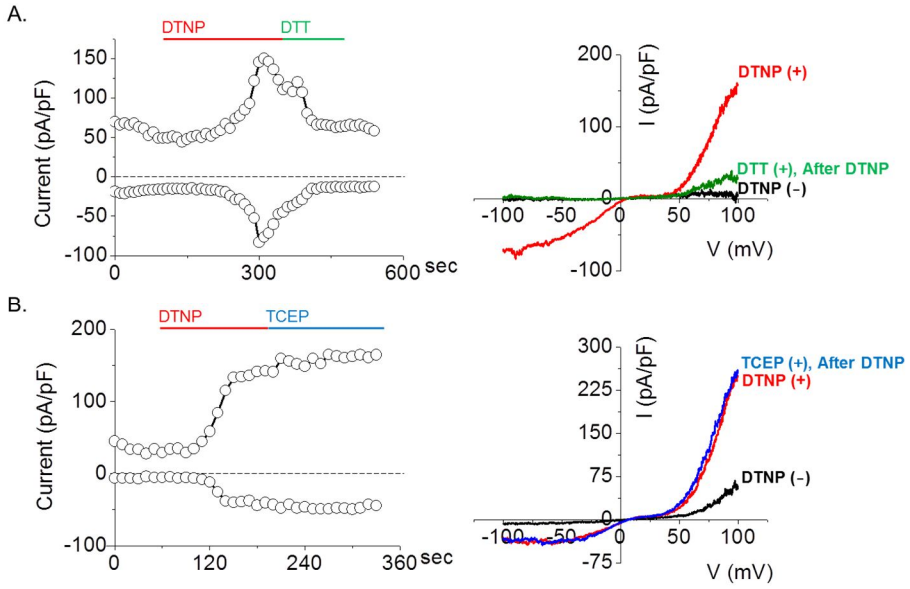

Fig. 3 Effects of reductants on DTNP−activated TRPC5 current
In hTRPC5−expressing HEK cells, TRPC5 currents were recorded under the condition of normal Tyrode solution. Four colored lines indicate application with DTNP (red), DTT (green), TCEP (blue), and basal current without the chemical (black) in current trace or Current (I)−Voltage (V) relationship.

A. ***Left***, A representative current trace of 30 μM DTNP−activated TRPC5 reversed by 10 mM DTT. ***Right***, A decreased $I-V$ curve of a typical doubly rectifying TRPC5 by DTT after DTNP activation.

B. ***Left***, A representative current trace of 30 μM DTNP−activated TRPC5, not affected by 1 mM TCEP. ***Right***, A remained $I-V$ curve of a typical doubly rectifying TRPC5 by TCEP after DTNP activation.

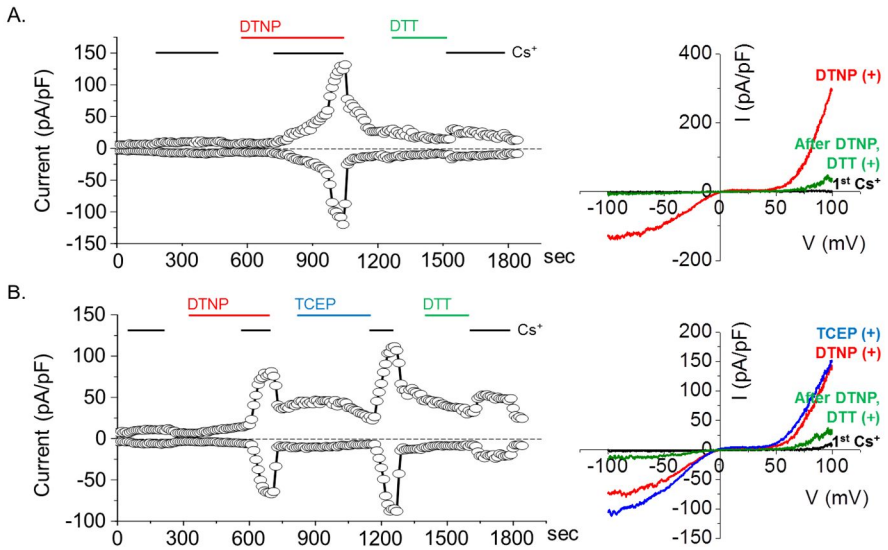

Fig. 4 Effects of reductants on DTNP-activated TRPC4β current
In mTRPC4β-expressing HEK cells, TRPC4β currents were recorded under the condition of 140 mM $[Cs^+]_o$ solution. Four colored lines indicate application with DTNP (red), DTT (green), TCEP (blue), and 1st Cs^+ current without the chemical (black) in current trace or Current (*I*)-Voltage (*V*) relationship.

A. ***Left***, A representative current trace of 30 μM DTNP-activated TRPC4β reversed by 10 mM DTT. ***Right***, A decreased *I*-*V* curve of a typical doubly rectifying TRPC4β by DTT after DTNP activation.

B. ***Left***, A representative current trace of 30 μM DTNP-activated TRPC4β, not affected by 1 mM TCEP. ***Right***, A remained *I*-*V* curve of a typical doubly rectifying TRPC4β by TCEP, but not DTT after DTNP activation.

Effects of redox agents on intracellular glutathione-dependent TRPC4/C5 activity

The intracellular distribution of glutathione is of great significance as ingeniously regulating in free radical scavenging and cellular detoxification for normal growth and metabolism. Free glutathione exists either in a reduced form with a free thiol group (GSH) or in an oxidized form with a disulfide between two identical molecules (GSSG). The redox status depends on the relative amounts of the reduced and oxidized forms of glutathione (GSH/GSSG). In normal conditions, the glutathione redox couple is present in concentrations between 1 and 10 mM, with the reduced GSH predominating over the oxidized form. In cells, the ratio exceeds 100, whereas in various models of oxidative stress this ratio was reported to decrease to values between 10 and 1 (25).

In most whole-cell experiments, the pipette solution largely resembles the ionic composition of the cytoplasm. But, unknown cytosolic factors relevant to the subject of study can be unwittingly washed out (26). Among intracellular cytosolic factors, glutathione (GSH) plays an essential role in protecting against reactive oxygen species (ROS). Thus, the presence of

GSH is important in order to prevent oxidized damage.

I asked whether intracellular GSH (reduced glutathione) attenuates cytosolic oxidation effect of TRPC5 by converting reactive disulfide (S−S) to thiol (−SH). When 3 mM GSH was infused in pipette solution, I identified weakened TRPC5 activation induced by DTNP (108 ± 19 pA/pF → 16 ± 9 pA/pF, Fig. 5A). Without GSH, the DTNP−induced activation in TRPC4β was 16.1 ± 5.9 pA/pF, whereas the current decreased to only 2.2 ± 0.8 pA/pF when GSH was included (Fig. 6A).

However, mixed disulfides including glutathionylated protein can be formed in response to changes in the GSH/GSSG ratio, or through a thiol/disulfide exchange between a protein sulfhydryl group and GSSG. This reaction removes GSSG, restoring the physiological redox conditions (27,28). However, elevated GSSG can oxidize, forming disulfide bonds with itself (GS−SG) or with protein thiols (PS−SG) (28). Thus, I asked whether the increased GSSG may act as oxidizing agents activating TRPC5 in the foregoing results. This was tested by infusing 2, 5 or 8 mM of GSSG. To efficiently observe GSSG response, I attempted a breakthrough (called “rupture”) for whole−cell mode on the recording after giga−seal formation,

because of rapid exchange from intracellular fluid to pipette solution with GSSG. Remarkably, the inclusion of 5 or 8 mM GSSG in pipette solution activated the TRPC5 current to 74 ± 13 or 132 ± 19 pA/pF compared to the control (2.1 ± 0.3 pA/pF) lacking GSSG. But, 2 mM GSSG hardly activated TRPC5 current (3.9 ± 0.9 pA/pF, Fig. 5B). Likewise, Cs^+ current of TRPC4β increased from 2.6 ± 0.8 pA/pF to 25.6 ± 5.9 pA/pF by 5 mM intracellular GSSG (Fig. 6B).

To further probe whether GSSG also induces TRPC5 activation via intracellular oxidation, I perfused with cell-permeable or impermeable reductant in extracellular solution. When treated with cell-permeable DTT in bath solution, GSSG-activated TRPC5 currents were significantly decreased from 60 ± 11 pA/pF to 11 ± 5 pA/pF (Fig. 5C). As Figure 3, TRPC5 activation by intracellular GSSG was no difference between normal Tyrode solution with or without 1 mM TCEP (60 ± 11 pA/pF → 56 ± 19 pA/pF, Fig. 5C).

TRPC5 channel can assemble with TRPC1 channel as a heteromeric structure (29). So I identified TRPC1α-TRPC5 activity by DTNP and GSSG. In Fig. 6C, I observed La^{3+}-induced outward current in TRPC1α-TRPC5 channel. DTNP

and GSSG also activated TRPC1α−TRPC5 channel (Fig. 6D,E).

To identify if TRPM2 channel is activated not only H_2O_2 (30), which has been reported previously, but also GSSG and DTNP, I first recorded the linear (ohmnic) current of TRPM2 activated by intracellular adenosine diphosphate ribose (cADPR) in hTRPM2−expressing HEK cell as a positive control. However, treatment with GSSG or DTNP showed no activation of TRPM2 (Fig. 6F).

These results suggest that similarly oxidants, the elevated GSSG activates TRPC4β or C5, independently of TRPM2, as a novel activator. This GSSG activation is adversely mediated in cytosolic oxidation under abnormal glutathione homeostasis, even if antioxidants such as reduced glutathione (GSH) regulate redox reaction by eliminating oxidizing substances. I tried to determine whether this reaction occurs directly in intracellular free cysteine (−SH) of TRPC channels.

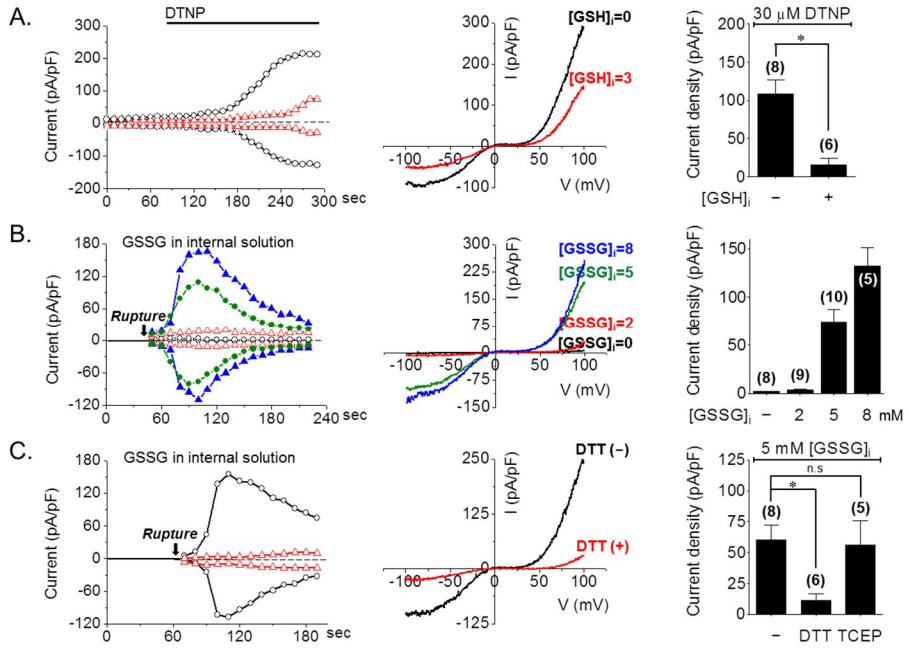

Fig. 5 Effects of redox agents on intracellular glutathione-dependent TRPC5 activity

In hTRPC5-expressing HEK cells, TRPC5 currents were recorded under the condition of normal Tyrode solution. In bar graph, the number indicates the recorded cell numbers (*N*) with patch clamp. Statistics of results is shown as $*P<0.05$ or no significance (n.s).

A. ***Left***, A representative current trace of 30 μM DTNP-activated TRPC5 attenuated by internally infused 3 mM GSH. ***Middle***, A decreased *I-V* curve of a typical doubly rectifying DTNP-activated TRPC5 by GSH. ***Right***, A summarized bar graph of inward current amplitudes of DTNP-activated TRPC5 by GSH at −60 mV. Two colored lines indicate application with 0 mM (black) and 3 mM (red) GSH in current trace or *I-V* curve.

B. ***Left***, A representative current trace of TRPC5 activated by GSSG. ***Middle***, A *I-V* curve of a typical doubly rectifying TRPC5 by GSSG. ***Right***, A summarized bar graph of inward

current amplitudes of TRPC5 by various GSSG concentrations at −60 mV. Four colored lines indicate application with 0 mM (black), 2 mM (red), 5 mM (green), and 8 mM GSSG (blue) in current trace or $I-V$ curve.

C. ***Left***, A representative current trace of 5 mM GSSG-activated TRPC5 attenuated by externally pretreated 10 mM DTT. ***Middle***, A decreased $I-V$ curve of a typical doubly rectifying GSSG-activated TRPC5 by DTT. ***Right***, A summarized bar graph of inward current amplitudes of DTNP-activated TRPC5 by DTT and 1 mM TCEP at −60 mV. Two colored lines indicate application without a reductant (black), with DTT (red), and TCEP (not shown) in current trace or $I-V$ curve.

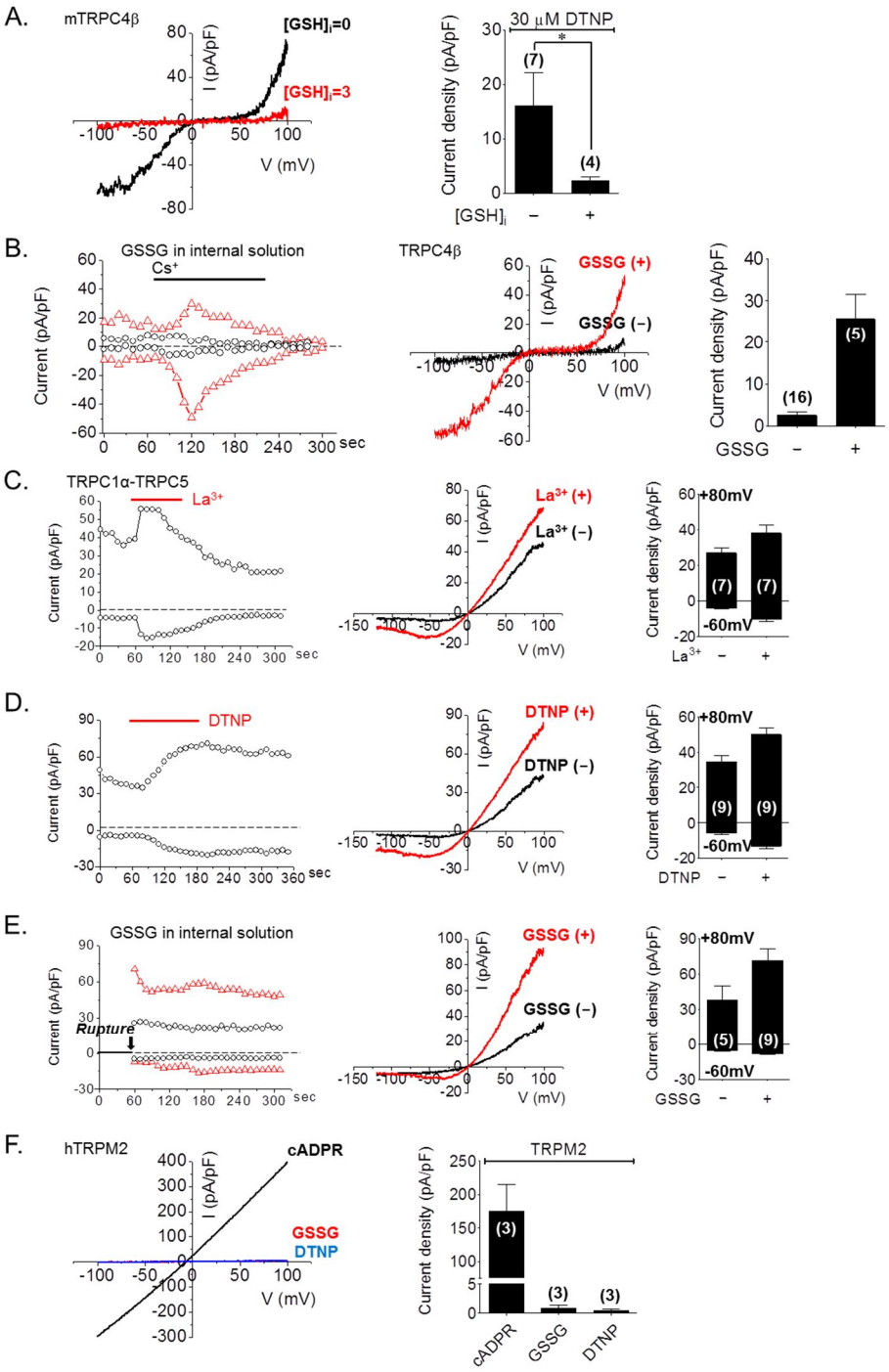

Fig. 6 Effects of redox agents on intracellular glutathione-dependent TRPC1 α, TRPC4β, and TRPM2 activity

In mTRPC4β-expressing HEK cells, TRPC4β currents were recorded under the condition of 140 mM $[Cs^+]_o$ solution. In bar

graph, the number indicates the recorded cell numbers (*N*) with patch clamp. Statistics of results is shown as $*P<0.05$ or no significance (n.s).

A. ***Left***. A decreased *I*−*V* curve of a typical doubly rectifying DTNP−activated TRPC4β by internally infused 3 mM GSH. ***Right***. A summarized bar graph of inward current amplitudes of DTNP−activated TRPC4β by GSH at −60 mV. Two colored lines indicate application with 0 mM (black) and 3 mM (red) GSH in *I*−*V* curve.

B. ***Left***, A representative current trace of TRPC4β activated by 5 mM GSSG. ***Middle***, A *I*−*V* curve of a typical doubly rectifying TRPC4β by GSSG. ***Right***, A summarized bar graph of inward current amplitudes of TRPC4β by GSSG at −60 mV. Two colored lines indicate application with 0 mM (black) and 5 mM (red) GSSG in current trace or *I*−*V* curve.

C. ***Left***, A representative current trace of TRPC1α−TRPC5 heteromeric channel activated by 200 μM La^{3+}. ***Middle***, A *I*−*V* curve of a outwardly rectifying TRPC1α−TRPC5 by La^{3+}. ***Right***. A summarized bar graph of inward and outward current amplitudes of TRPC1α−TRPC5 by La^{3+} at −60 mV and +80 mV, respectively. Two colored lines indicate application with 0 μM (black) and 200 μM (red) La^{3+} in current trace or *I*−*V* curve.

D. ***Left***. A representative current trace of TRPC1α−TRPC5 heteromeric channel activated by 30 μM DTNP. ***Middle***, A *I*−*V* curve of a outwardly rectifying TRPC1α−TRPC5 by DTNP. ***Right***, A summarized bar graph of inward and outward current amplitudes of TRPC1α−TRPC5 by DTNP at −60 mV and +80 mV, respectively. Two colored lines indicate application with 0 μM (black) and 30 μM (red) DTNP in current trace or *I*−*V* curve.

E. ***Left***, A representative current trace of TRPC1α−TRPC5 heteromeric channel activated by 5 mM GSSG. ***Middle***, A *I*−*V* curve of a outwardly rectifying TRPC1α−TRPC5 by GSSG. ***Right***, A summarized bar graph of inward and outward current amplitudes of TRPC1α−TRPC5 by GSSG at −60 mV and +80 mV, respectively. Two colored lines indicate application with 0 mM (black) and 5 mM (red) GSSG in current trace or *I*−*V* curve.

F. ***Left***. A linear (ohmnic) *I*−*V* curve of hTRPM2 activated by 300 μM cADPR, not activated by 5 mM GSSG, or 30 μM DTNP. ***Right***. A summarized bar graph of linear current amplitudes of TRPM2 by cADPR, GSSG, and DTNP at −60 mV. Three colored lines indicate application with cADPR (black), GSSG (red), and DTNP (blue) in *I*−*V* curve.

The activation of TRPC4/C5 through cytosolic cysteine directly modified by oxidized glutathione (GSSG)

Oxidative stress induces oxidative damage to DNA, lipids and proteins. The oxidation in protein can mostly occur with thiol groups in cysteine. The susceptibility of cysteinyl residues to redox reactions is influenced by the accessibility of the thiol within the three-dimensional structure of the protein and the cysteine reactivity (31). GSSG can cause protein S-glutathionylation of a post-translational modification under an appropriate GSH/GSSG ratio. Most cysteine modifications are unstable and can easily be reversed (32). The reversibility of this process is mediated by direct thiol/disulfide exchange reactions with GSH (27).

Of TRPC group, TRPC1, 4, and 5 have similar homology of the sequence with highly conserved cysteines, especially in NH_2-terminal domain. I aligned the sequence for TRPC1, C4, and C5 (Table 1).

In order to determine whether covalent modification by GSSG is based on free sulfhydryl (-SH) group of cysteine residue in TRPC channels, I investigated 8 cysteine mutants and a deletion mutant of mouse TRPC5 which were kindly provided by Yasuo

A. The homology of TRPC5(Mouse), TRPC4(Mouse), and TRPC1(Mouse)

Table 1 Alignment of the full sequences on mTRPC1, mTRPC4, and mTRPC5 channels.

Mori (14). GSSG-activated current densities (pA/pF) of single mutants; C65S, C176S, C178S, C181S, C248S, C307S, C682S, and C956S were 54 ± 11 pA/pF, 7.3 ± 2.2 pA/pF, 5.8 ± 2.1 pA/pF, 1.2 ± 0.2 pA/pF, 49 ± 9 pA/pF, 51 ± 10 pA/pF, 70 ± 11 pA/pF and 80 ± 28 pA/pF, respectively. The wild type or deletion mutant (Δ764~954 a.a) including 8 cysteine at position 804, 809, 877, 895, 920, 924, 930, and 935 in mouse TRPC5 was 75 ± 9 pA/pF or 90 ± 11 pA/pF, respectively (Fig. 7B, *left*). To examine whether one or more cysteines are involved in sulfhydryl modification, I made multiple cysteine mutants by changing another cysteine to serine from the mutants provided by Mori (14) using site-directed mutagenesis in my hands. N-terminus (1.2 ± 0.3 pA/pF) or intracellularly whole cysteines mutant (0.7 ± 0.2 pA/pF) had no current. However, C-terminus cysteines mutant (109 ± 26 pA/pF) with deletion was not significantly different from the current of wild type (97 ± 12 pA/pF, Fig. 7B, *right*).

After all, I predicted the putative S-glutathionylated site at position 176 and 178 through trial and error. C176S-C178S double mutant (3.8 ± 1.0 pA/pF) was not activated by GSSG compared to the wild type (60 ± 13 pA/pF, Fig. 7C). And also,

C176S-C178S mutant (1.2 ± 0.3 pA/pF) of mouse TRPC4β was unaffected by GSSG in comparison to the wild type (17.5 ± 4.4 pA/pF, Fig. 8D). To check whether TRPC5 is directly glutathionylated by oxidized form and for quantitative analysis of predicted double mutant (C176S-C178S), I identified the S-glutathionylated TRPC5 interacting with glutathione using co-Immunoprecipitation (Co-IP) assay. In Figure 7D, wild type TRPC5 apparently interacted with 5 mM GSSG, but not C176 and C178 mutant of mouse TRPC5. Interestingly, endogenous glutathione was partially bound to TRPC5 (WT) without pretreating with GSSG.

I asked that N-terminus cysteine mutant of TRPC4/C5 should be activated by other activation systems (ex. Lanthanides (33), Cesium (34), GTPγS (a stable analogue of guanosine triphosphate) (35), etc. which is irrelevant to oxidation process, even if it changed the cysteine involving in oxidation to serine. Both of WT and C176S-C178S mutant of TRPC5 were activated by 200 μM La^{3+}, stabilizing the open state of the channels (Fig 7C, *filled bar*). With or without GTPγS activating GTPases such as G-protein coupled receptors (GPCRs) or small GTP binding protein, Cs^{+} current of C176S-C178S

mutant was significantly indifferent compared to wild type of TRPC5 (Fig. 8A). Interestingly, some cysteines including C181 are critical to channel trafficking and stabilization via S-palmitoylation (data not shown). To rule out this process in C176 and C178, I assayed surface expression of WT and C176S-C178S by performing surface biotinylation (Fig. 8B).

These results imply that TRPC4β or TRPC5 is directly glutathionylated by GSSG and the gating of TRPC4β/C5 involves two intracellular cysteines at positions 176 and 178 that is conserved in TRPC1/C4/C5 and lies near ankyrin repeat domain (ARD) in NH_2-terminus.

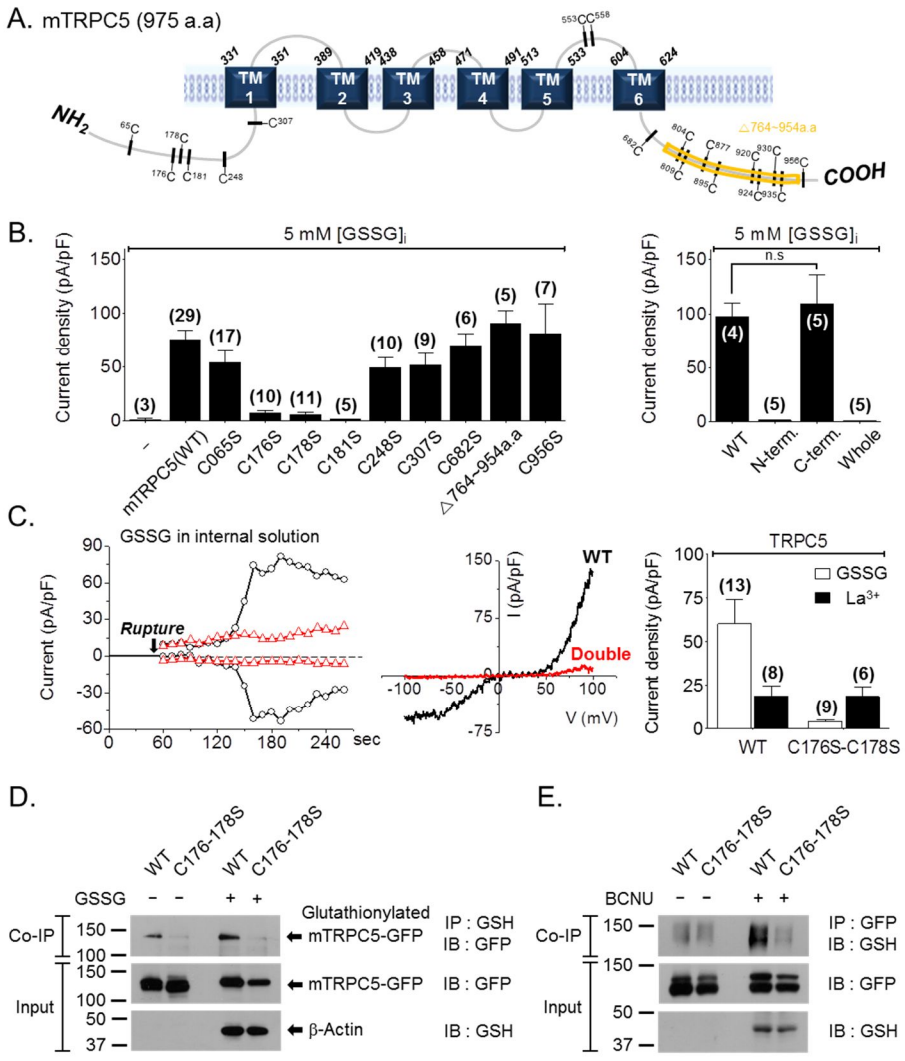

Fig. 7 The activation of TRPC5 through cytosolic cysteine directly modified by oxidized glutathione (GSSG)

All experiments were performed in mTRPC5-expressing HEK cells. In bar graph, the number indicates the recorded cell numbers (*N*) with patch clamp. Statistics of results is shown as $*P<0.05$ or no significance (n.s).

A. Cysteine residues mapped on mouse TRPC5

B. A summarized bar graph of inward current amplitudes of TRPC5 mutants (***Left***, single or ***Right***, multiple cysteine, and deletion) by 5 mM GSSG at −60 mV, compared to wild type

(WT).

C. ***Left***, A representative current trace of TRPC5 (WT or C176S-C178S) induced by 5 mM GSSG. ***Middle***, A $I-V$ curve of a typical doubly rectifying TRPC5 (WT or C176S-C178S) by GSSG. ***Right***, A summarized bar graph of inward current amplitudes of TRPC5 (WT or C176S-C178S) by GSSG (*open bar*) or 200 μM La^{3+} (*filled bar*) at −60 mV. Two colored lines indicate the current of transient transfected cells with WT (black) and C176S-C178S double mutant (red) of mouse TRPC5 in current trace or $I-V$ curve.

D. S-glutathionylation of TRPC5 (WT or C176S-C178S) with and without GSSG treatment. IP, immunoprecipitation.

E. S-glutathionylation of TRPC5 (WT or C176S-C178S) with and without BCNU treatment.

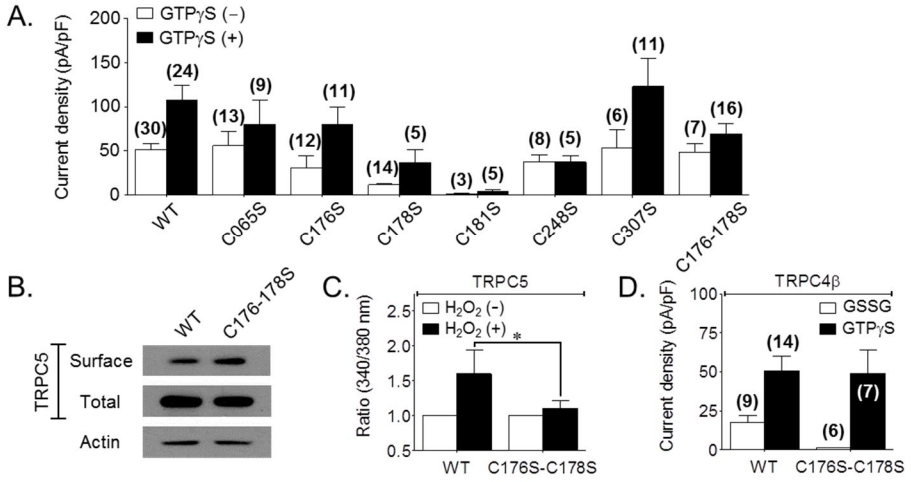

Fig. 8 The activation of TRPC4β/C5 through cytosolic cysteine directly modified by oxidized glutathione (GSSG)

All experiments were performed in mTRPC5 or mTRPC4β-expressing HEK cells. In bar graph, the number indicates the recorded cell numbers (*N*) with patch clamp. Statistics of results is shown as $*P<0.05$ or no significance (n.s).

A. A summarized bar graph of inward current amplitudes of TRPC5 mutants (single or double cysteines) under infusion with 0.2 mM GTPγS (*filled bar*) or without GTPγS (*open bar*) at −60 mV, compared to wild type (WT).

B. A representative surface expression level of TRPC5 (WT or C176S-C178S). Surface expression of TRPC5 was determined by surface biotinylation, compared to total TRPC5 expression. TRPC5 was detected with anti-GFP.

C. A summarized bar graph of intracellular Ca^{2+} fluorescence intensity by 1 mM H_2O_2 in TRPC5 (WT or C176S-C178S)-expressing HEK cells through fluorescent $[Ca^{2+}]_i$ measurements technique using the Fura-2 at 340 / 380 nm.

D. A summarized bar graph of inward current amplitudes of TRPC4β (WT or C176S-C178S) by 5 mM GSSG (*open bar*) or 0.2 mM GTPγS (*filled bar*) at −60 mV.

Effects of glutathione reductase inhibitor (BCNU) and peroxidase inhibitor (BSO) in clonal striatal cell lines from mutant huntingtin knock-in mice

It is well-known that TRPC channels are densely expressed in mammalian brain, such as corticolimbic brain region like the hippocampus, prefrontal cortex and lateral septum (12,36) and already reported that reduced antioxidant activity induced apoptosis of neuron cell in neurodegenerative diseases (37).

For that reason S-glutathionylation in TRPC channels may negatively contribute to Huntington's disease, I firstly applied western blotting and reverse transcription-polymerase chain reaction (RT-PCR) analysis for detection of TRPC4/C5 in striatal cells. I identified that TRPC4/C5 are endogenously expressed in clonal striatal cell lines from wild-type (ST*Hdh*$^{Q7/7}$) and mutant huntingtin knock-in (ST*Hdh*$^{Q111/111}$) mice (Fig. 9A/Fig. 10A,B).

To show glutathione-dependent cell viability in HD cell line, I used carmustine (1,3-bis(2-chloroethyl)-N-nitrosourea) (BCNU) or L-buthionine (S,R) sulfoximine (BSO), causing shift in the level of intracellular GSH redox balance towards the oxidized form (GSSG) or depletion in total glutathione level,

respectively (Fig. 9B). A 6-hour exposure to 100 μM BCNU or 48-hour exposure to 100 μM BSO decreased both of the viability of ST*Hdh*$^{Q7/7}$ (Q7/7) and ST*Hdh*$^{Q111/111}$ (Q111/111) cells compared to the one that pretreated with each vehicle (Fig 9C). When stained with trypan blue as a marker for dead cells, BCNU (Fig. 9D) or BSO (Fig. 10C) increased necrotic cells. To determine whether BCNU or BSO effect is dependent on intracellular GSH to increase cell toxicity, I used N-acetyl-L-cysteine (NAC) as a precursor to glutathione to increase intracellular GSH level. NAC diminished in the toxicity of intracellular GSSG caused by BCNU (Fig. 9E) or BSO (Fig. 10D). In order to investigate whether GSSG leads to apoptosis resulting in cell death, I analyzed 6-hour incubation to BCNU-pretreated cells using flow cytometry analysis after doubly staining a cell population with propidium iodide (PI) and Annexin V which are able to distinguish between early or late apoptosis and necrosis. In Q111 cells, apoptotic cells were increased by BCNU from 5.9 ± 1.2 % to 12.7 ± 1.5 % more than double (Fig. 9F), indicating minor modality of apoptosis in Q7 (Fig. 10E). I asked that GSH depletion is more vulnerable to oxidative stress. This was tested by addition of H_2O_2 in

condition of GSH depletion by BSO. When pretreated with 20 μM H_2O_2 for 24h after 100 μM BSO preincubation to deplete intracellular glutathione for 24h, hydrogen peroxide (H_2O_2) in combination with BSO enhanced reduction in the cell viability of both cell lines (Fig. 9G). To calculate the inhibitory concentration 50% (IC_{50}), I pretreated with a series of H_2O_2 in dose dependent manner. In Q7 or Q111, the IC_{50} value for H_2O_2 decreased from 10^2 μM<IC_{50}<10^3 μM (in the absence of BSO) to 38 or 35 μM (in the presence of BSO), respectively (Fig. 10F,G).

I next asked whether calcium signaling is enough to contribute to cell death during BCNU incubation. I measured FRET efficiency of Yellow Cameleon 6.1 (YC 6.1) as a calcium sensor which detects Ca^{2+} mobilization in cytosol with Foester resonance energy transfer (FRET) technique. In transfected cell with YC6.1, BCNU sustainedly increased basal Ca^{2+} level as time went on (Fig. 9H). I observed maximum value (32.2 ± 1.1 %) of YC 6.1−FRET signal with BCNU in Q111 within 90 min. In contrast, Q7 cells increased by ~35.0 ± 3.1 % after 180 min of BCNU treatment, indicating that Q7 is more resistant to oxidative stress than Q111 (Fig. 9I). And also basal Ca^{2+} level

in Q111 than Q7 cells remained slightly high. But BSO-induced intracellular Ca^{2+} was not statistically significant at the 25% FRET signal (24.3 ± 0.6 % → 26.8 ± 1.6 %) in Q111 (Fig. 10H,I).

These results imply that BCNU treatment in turn induces intracellular GSH depletion, elevated GSSG, increased intracellular Ca^{2+} level, and Ca^{2+}-dependent apoptosis in HD cell line, considering that intracellular GSSG activates TRPC channels. Regardless of glutathione, newly produced ROS mediates (ex. hydrogen peroxide, nitric oxide, etc.) can damage neuron cells via elevated and sustained Ca^{2+} in cytosol under impaired antioxidants activity.

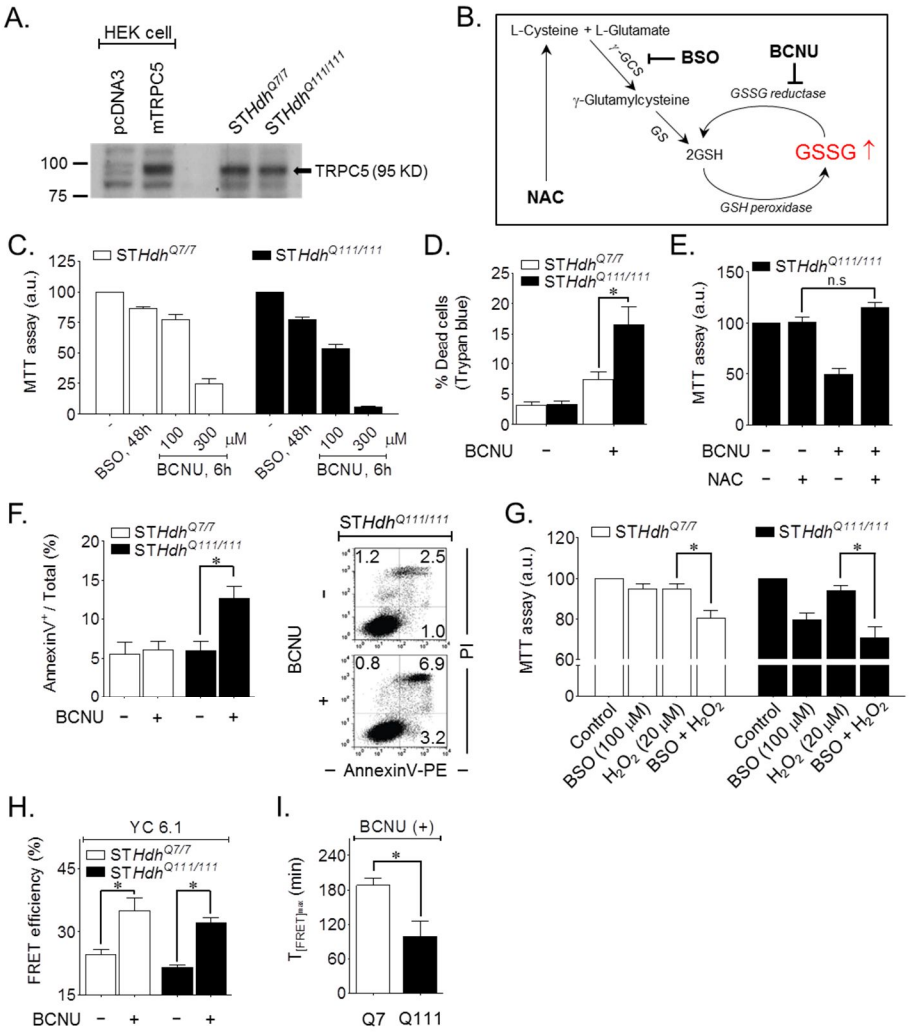

Fig. 9 Effects of glutathione reductase inhibitor (BCNU) and peroxidase inhibitor (BSO) in clonal striatal cell lines from mutant huntingtin knock-in mice

All experiments were performed in ST*Hdh*$^{Q7/7}$ (Q7) and ST*Hdh*$^{Q111/111}$ (Q111) cells unless otherwise stated.

A. Expression pattern of TRPC5 in Q7 and Q111 cells by western blotting for identification of endogenous protein. Transient transfection with mTRPC5 in HEK cells was shown as a control.

B. Schematic diagram of glutathione circuits and mechanisms of related drugs (BCNU, BSO, NAC). GSSG reduction to GSH,

which is blocked by BCNU, leads to increasing intracellular stores of [GSSG]. The formation of GSH by the action of γ–glutamylcysteine synthetase (γ–GCS) is blocked by BSO, inducing total glutathione depletion. NAC elevates [GSH] as a precursor of glutathione.

C–G. Cell viability changes of Q7 and Q111, resulting from BCNU or BSO treatment.

C. After 100 μM BSO (48h) and 100 μM or 300 μM BCNU (6h) treatment, live cells are indicated by MTT. (BSO; N=22, 100 μM BCNU; N=8, 300 μM BCNU; N=8)

D. After 100 μM BCNU (6h) treatment, dead cells are indicated by stained cell counting with trypan blue. (N=12, $*P$<0.05)

E. Under pretreatment with 5 mM NAC (24h) prior to treatment with 100 μM BCNU (6h), Q111 live cells, but not Q7 (not shown), are indicated by MTT. (N=10, n.s, no significance)

F. **Left**, A summarized bar graph of 100 μM BCNU (6h)–caused apoptotic death in Q7 and Q111 cells by FACS analysis. (N=4, $*P$<0.05) ***Right***, A representative FACS analysis scatter–grams of Annexin V and PI–stained Q111 by 100 μM BCNU (6h). BCNU treatment showed four different cell populations marked as; double negative (unstained) cells showing live cell population (*lower left*), Annexin V positive and PI negative stained cells showing early apoptosis (*lower right*), Annexin V/PI double–stained cells showing late apoptosis (*upper right*), and finally PI positive and Annexin V negative stained cells showing dead cells (*upper left*).

G. Under pretreatment with 100 μM BSO (24h) prior to treatment with 20 μM H_2O_2 (24h), live cells are indicated by MTT. (N=8, $*P$<0.05)

H–I. Ca^{2+} imaging of Q7 and Q111 using FRET–based cameleon (YC6.1), resulting from BCNU treatment.

H. A summarized bar graph of FRET signal by BCNU at the maximum peak value. (N=3, $*P$<0.05)

I. A summarized bar graph of required time of the maximum FRET value by BCNU. (N=3, $*P$<0.05)

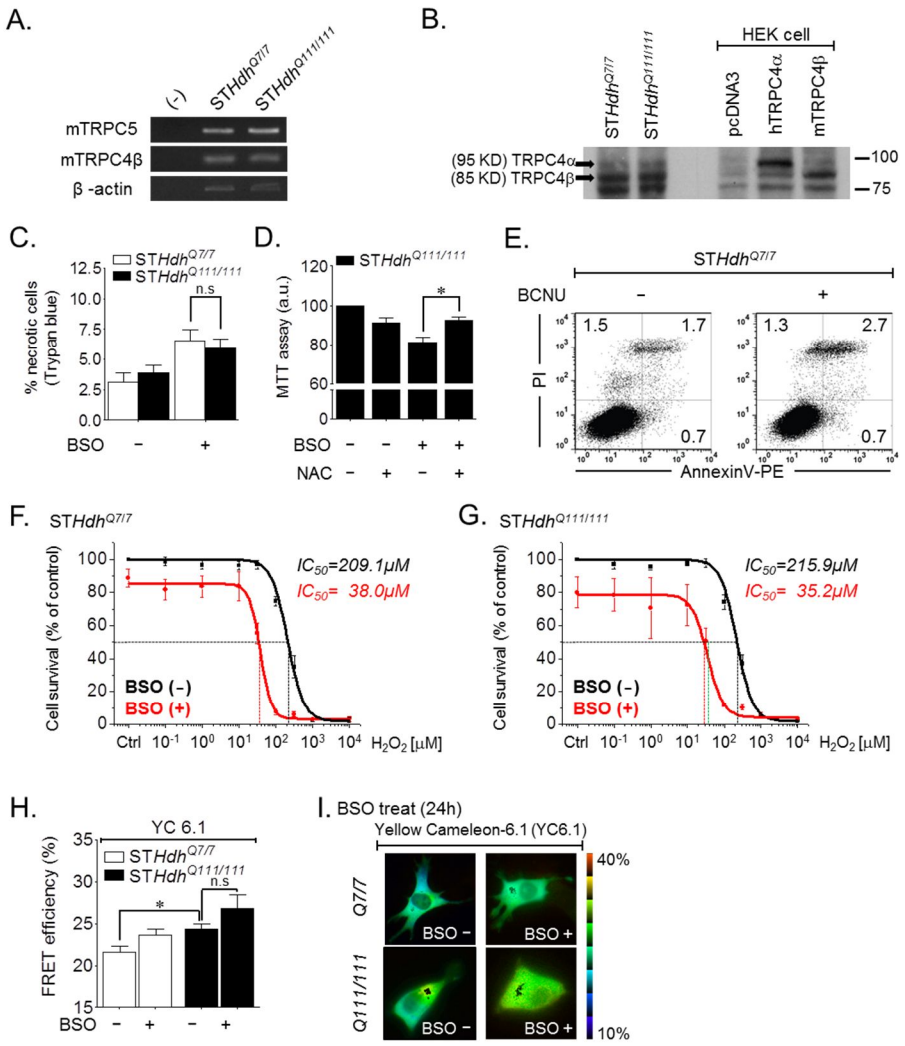

Fig. 10 Effects of glutathione reductase inhibitor (BCNU) and peroxidase inhibitor (BSO) in Q7 or Q111 cells

All experiments were performed in ST*Hdh*$^{Q7/7}$ (Q7) and ST*Hdh*$^{Q111/111}$ (Q111) cells unless otherwise stated.

A. Expression pattern of TRPC4β and TRPC5 in Q7 and Q111 cells by RT-PCR for identification of endogenous genes. β-Actin was also used as an internal control.

B. Expression pattern of TRPC4β in Q7 and Q111 cells by western blotting for identification of endogenous protein. Transient transfection with TRPC4α and TRPC4β in HEK cells was shown as a control.

C–G. Cell viability changes of Q7 and Q111, resulting from BCNU or BSO treatment.

C. After 200 μM BSO (24h) treatment, dead cells are indicated by stained cell counting with trypan blue. (N=6, $*P$<0.05)

D. Under pretreatment with 5 mM NAC (24h) prior to treatment with 200 μM BSO (24h), Q111 live cells, but not Q7 (not shown), are indicated by MTT. (N=10, n.s, no significance)

E. A representative FACS analysis scatter–grams of Annexin V and PI–stained Q7 by 100 μM BCNU (6h).

F. Cell viability changes of Q7 by dose–dependently treatment with H_2O_2 (24h) before and after 100 μM BSO (24h) application. Live cells are indicated by MTT. Dashed lines indicate IC_{50} of H_2O_2 with (red) or without BSO (black). (N=5, n.s, no significance)

G. Cell viability changes of Q111 by dose–dependently treatment with H_2O_2 (24h) before and after 100 μM BSO (24h) application. Live cells are indicated by MTT. Dashed lines indicate IC_{50} of H_2O_2 with (red) or without BSO (black). Green dashed line indicates IC_{50} of H_2O_2 under pretreatment with BSO in Q7 cells. (N=5, n.s, no significance)

H–I. Ca^{2+} imaging of Q7 and Q111 using FRET–based cameleon (YC6.1), resulting from BSO treatment.

H. A summarized bar graph of FRET signal by BSO at the maximum peak value. Data obtained from at least 15 cells for each condition from three different transfections. ($*P$<0.05, n.s, no significance)

I. A fluorescence image of cytoplasmic localization of YC6.1 in Q7 and Q111 cells before and after 200 μM BSO (24h) application. Cells represented in pseudo color scale.

TRPC5 as a mediator of cell death under abnormal glutathione in huntingtin mutant striatal cell

My new finding on TRPC5 S-glutathionylation suggests the possibility that cytosolic GSH pool directly causes neuronal damage in Huntington's disease. To determine whether Ca^{2+} mobilization by intracellular GSSG contributes to cell death, I down-regulated cytosolic Ca^{2+} mobilization with a broad antagonist of TRPCs and VOCCs (38), 10 μM cadmium chloride ($CdCl_2$). I first confirmed the blocking effect on TRPC5 with cadmium by patch clamp method (Fig. 11A). Remarkably, upon treatment of 10 μM Cd^{2+} to block TRPC channel before 24 hour of following treatment with 100 μM BCNU, Q7 or Q111 cells was sufficient to rescue BCNU-induced cell death (Q7; 83.8 ± 1.4 % → 100.9 ± 2.7 %, Q111; 61.2 ± 3.4 % → 74.5 ± 2.9 %, Fig. 11B). To further investigate specificity of TRPC5 in BCNU-induced apoptotic death, I used TRPC4/C5 specific inhibitor and transiently transfected small interfering RNA (siRNA) of TRPC5 for TRPC5 knockdown. As a selective and potent antagonist of TRPC4/C5 channel (39), ML204 blocked DTNP or GSSG-activated TRPC5 currents (Fig. 11C,D). This blocking effect on TRPC5 considerately attenuated BCNU-induced cell

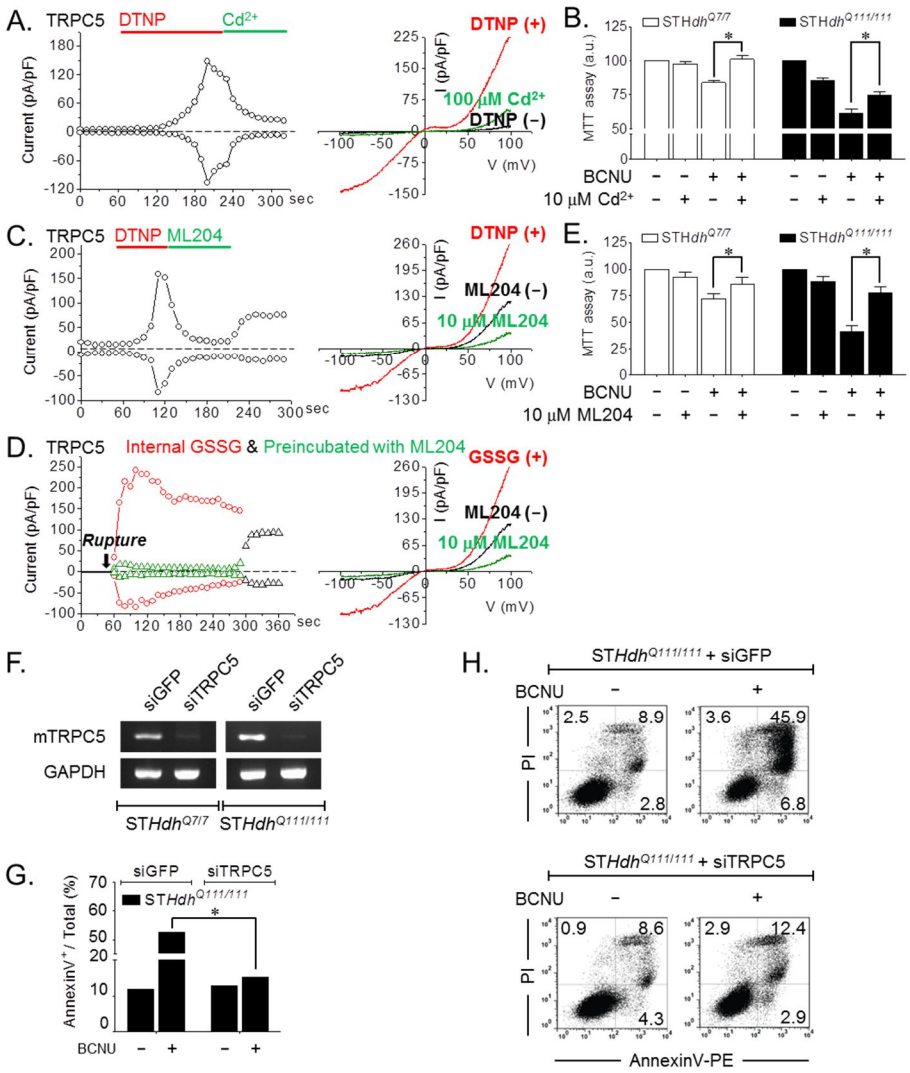

Fig. 11 TRPC5 as a mediator of cell death under abnormal glutathione in huntingtin mutant striatal cell

All experiments were performed in ST*Hdh*$^{Q7/7}$ (Q7) and ST*Hdh*$^{Q111/111}$ (Q111) cells unless otherwise stated.

A. In mTRPC5-expressing HEK cells, ***Left***, A representative current trace of 30 μM DTNP-activated TRPC5 blocked by 10 μM $CdCl_2$. ***Right***, A decreased *I-V* curve of a typical doubly rectifying DTNP-activated TRPC5 by $CdCl_2$.

B. Cell viability changes of Q7 and Q111 under pretreatment with 10 μM Cd^{2+} (24h) prior to treatment with 100 μM BCNU (6h). Live cells are indicated by MTT. (Q7; *N*=7,

Q111; N=9, $*P<0.05$)

C. In mTRPC5-expressing HEK cells, ***Left***, A representative current trace of 30 μM DTNP-activated TRPC5 blocked by 10 μM ML204. ***Right***, A decreased $I-V$ curve of a typical doubly rectifying DTNP-activated TRPC5 by ML204.

D. In mTRPC5-expressing HEK cells, ***Left***, A representative current trace of 5 mM GSSG-activated TRPC5 blocked by 10 μM ML204. ***Right***, A decreased $I-V$ curve of a typical doubly rectifying GSSG-activated TRPC5 by ML204.

E. Cell viability changes of Q7 and Q111 under pretreatment with 10 μM ML204 (18h) prior to treatment with 100 μM BCNU (6h). Live cells are indicated by MTT. (Q7; $N=5$, Q111; N=5, $*P<0.05$)

F. Knockdown of gene expression by TRPC5 siRNA in Q7 and Q111. RT-PCR was performed to analyze knockdown of endogenous genes by siTRPC5. siGFP cells transfected with a control GFP siRNA, and GAPDH was also used as an internal control.

G. A summarized bar graph of 100 μM BCNU (6h)-caused apoptotic death in Q111 cells after TRPC5 knockdown. ($N=1$)

H. A representative FACS analysis scatter-grams of Annexin V and PI-stained Q111 under knockdown with siGFP or siTRPC5 (48h) prior to treatment with 100 μM BCNU (6h).

death (Q7; 72.1 ± 5.1 % → 85.9 ± 6.7 %, Q111; 41.2 ± 5.7 % → 77.6 ± 5.8 %, Fig. 11E). As shown in Figure 11F, I performed to analyze knockdown of endogenous TRPC and identified silencing of TRPC5 gene using reverse transcription polymerase chain reaction (RT-PCR). When pretreated with 100 μM BCNU for 6h after 10 nM siGFP or siTRPC5 transfection for 48h, siTRPC5 significantly attenuated BCNU-induced cell death (Fig. 11G,H).

These results imply that BCNU treatment in turn induces intracellular GSH depletion, elevated GSSG, increased intracellular Ca^{2+} level, and Ca^{2+}-dependent apoptosis in HD cell line, considering that intracellular GSSG activates TRPC channels. Regardless of glutathione, newly produced ROS mediates (ex. hydrogen peroxide, nitric oxide, etc.) can damage neuron cells via elevated and sustained Ca^{2+} in cytosol under impaired antioxidants activity.

As previously reported, Ca^{2+} influx through TRPM2 is linked to neuroinflammatory response in human microglia and astrocytes (40). Furthermore, my results imply that TRPC5 as a source of Ca^{2+} can contribute to oxidative stress-induced damage in striatal cells under abnormal glutathione homeostasis.

In summary, I clarified the role of TRPC5 in Huntington's disease, showing that the neuronal apoptosis is caused by abnormal cytosolic Ca^{2+} influx through TRPC5. I further demonstrated a novel TRPC5 activation mechanism that cytosolic GSSG oxidizes to protein S-glutationylation (PSSG) in TRPC5.

DISCUSSION

Glutathione (GSH) is the most abundant thiol antioxidant in mammalian cells and maintains thiol redox in the cells. Oxidized glutathione (GSSG) glutathionylates the cysteine in the active enzymatic site with an appropriate GSH/GSSG ratio (4,5,17,25,27,28). Glutathione, which "adds" itself onto regulatory molecule, "glutathionylates" many proteins (enzyme, receptors, structural proteins) that carry on phosphorylation and dephosphorylation of proteins. S-glutathionylation is a post-translational modification mechanism occurring in a variety of physiological or pathophysiological conditions (41). It is widely acknowledged that changes in the cellular reduced/oxidized glutathione ratio trigger signal transduction mechanisms affecting cell survival. GSSG is capable of causing protein S-glutathoinylation of reversible formation of protein mixed disulfides (protein-SSG). Post-translational reversible S-glutathionylation is known to regulate signal transduction as well as activities of several redox sensitive thiol-protein (42,43). Elevated cellular GSSG levels result in rapid cellular response to moderate oxidative stress and may directly

influence on cell death. To address this question, I used whole-cell patch clamp and the preincubation of BCNU to raise cellular GSSG or GSH as control to investigate the significance of GSSG on cell death. My results show that TRPC5 channels are strongly activated under oxidative stress by S-glutathionylation at Cys176 (C176) and Cys178 (C178) residues of the TRPC5.

Excessive reactive oxygen species produced during oxidative stress result in structural modification of proteins affecting protein function (44). Although some studies showed that the TRPC5 channel are targeted by redox regulation, data are inconsistent regarding the effect of oxidants or thiol oxidation on TRPC5 channel from different research groups. TRPC channel was activated via cysteine S-nitrosylation (14) or breakage of disulfide bridge (15) at Cys553 (C553) and Cys558 (C558). Contrary to Xu et al. (15), the activation of TRPC5 by DTT may be caused by ER stress-induced cytosolic Ca^{2+} effect. Unlike C176 and C178 as a putative S-glutathionylation site, C553 and C558 do not seem to be involved in S-glutathionylation. In TRPC5 channel, the mutation of C553 and C558 results in an absence of ionic currents

although the channels are still expressed. C553 and C558 are located on the extracellular interface of the cellular membranes, accessible to extracellular environments. The accessibility of this residue to extracellular oxidants as well as membrane-impermeable PDS, but not intracellular GSSG, suggests that C553 and C558 could be a site for extracellular redox modulation rather than intracellular S-glutathionylation. Similar results were obtained Kir channels. In the Kir2.1 channel, the mutation of Cys122 (C122) results in an absence of ionic currents although the channels are still expressed (45,46). Yang et al. (2011) was able to record the currents from the C120S mutant in Kir6.1, the counter part of Cys122 in Kir2.1, althrough the currents were small compared to most of the other mutants (47). Based on the Kir protein structure, C120 in Kir6.1 is located on the extracellular interface of the cellular membranes, having an access to extracellular environments. The accessibility of this residue to extracellular oxidants as well as membrane-impermeable PDS, but not intracellular GSSG, proposed that C120 of Kir6.1 could be a site for extracellular redox modulation rather than intracellular S-glutathionylation. Therefore intracellular cysteines of TRPC5,

but not C553 or C558, have prominent sensitivity to oxidants.

This cytosolic oxidation activates TRPC5 channels by modulating from sulfhydryl group (−SH) of cysteine to glutathionylated cysteine (protein−SSG), nitrosylated cysteine (protein−SNO), and hydroxylated cysteine (protein−SOH) by GSSG, NO, and H_2O_2, respectively. However internal GSSG or external DTNP did not activate TRPM2 channel since TRPM2 oxidation is activated by modification from methionine (−S−CH_3) to sulfoxide (protein−SO−CH_3) or sulfone (protein−SOO−CH_3)(11). Although S−glutathionylation was detected in TRPC5 homomeric channels by directly adding GSSG (Fig. 7D) or preincubating BCNU via Co−IP (Fig. 7E), this reaction in TRPC1/C4/C5 homo− or heteromeric channels might occur at similar conserved cysteine 176 and 178 as shown by activation in these channels via patch clamp (Fig. 6).

This protein modulation mechanism is remarkable especially in vasculatures because oxidative stress is a major contributing factor to several cardiovascular diseases, in which *S*−glutathionylation plays an important role (44). Dysregulation of cytosolic glutathione homeostasis is also a common feature of neuropathic pain and neurodegenerative disorders (1).

The oxidation process is a normal byproduct of intracellular metabolism. The produced free radicals damage the body's cells and organs. The brain is particularly vulnerable to oxidative stress due to high energy needs and oxygen consumption compared to other organs. Thus, high antioxidant activity in nerve system is essential for elaborate regulation to remove free radicals. However, the abnormal glutathione homeostasis in neuron leads to the formation of reactive oxygen species. Subsequently the accumulation of oxidized glutathione (GSSG) results in the protein oxidation that is fatal to cells. At early stages of the Huntington's disease (HD), polyQ-expanded Htt (Htt^{exp}) may be directly linked to excitotoxicity and activation of Ca^{2+}-dependent proteases by altered Ca^{2+} homeostasis. Proteolytic processing of mutant Htt and abnormal calcium signaling may be responsible for disease progression and pathogenesis (48). Calcium homeostasis disruption in HD implicates several mechanisms, such as alterations of calcium buffering capacities, deregulation of calcium channel activities, or excitotoxicity. The decreased calbindin-D28K expression of some calcium buffering protein may be particularly affected in the disease (49). The Htt^{exp} sensitizes not only N-methyl-D-

aspartate receptor 2B and metabotropic glutamate receptor 1/5 in brain, leading to enhanced Ca^{2+} influx following receptor stimulation (48,50,51,52) but also endoplasmic reticulum type 1 inositol (1,4,5)-trisphosphate receptor leading to enhanced Ca^{2+} release following metabotropic glutamate receptors class 1/5 activation (53). Due to malfunctions of mitochondria as a calcium regulator, mutant Htt protein significantly decreased the calcium threshold necessary to trigger mitochondrial permeability transition (MPT) pore opening (54,55,56). Furthermore, glutamate toxicity is a major contributor to pathological neuron cell death and is known to be mediated by reactive oxygen species and GSH loss (57,58).

Given that glutathione-depleted state by oxidative glutamate neurotoxicity impairs cellular antioxidant defenses resulting in oxidative stress, TRPC4/C5 may contribute to oxidative stress-induced Ca^{2+} source in HD. To address this question, I investigated whether BCNU-induced cell death is associated with TRPC5 and Ca^{2+} using clonal striatal cell lines from wild-type (ST*Hdh*$^{Q7/7}$) and mutant huntingtin knock-in (ST*Hdh*$^{Q111/111}$) mice. My results suggest that canonical or classical TRP channel, subtype C4 and C5, are enriched in the

striatum and may play a role in the dysregulation of Ca^{2+} in HD through extracellular Ca^{2+} influx or depolarizing the membrane potential by TRPC4/5 S-glutathionylation (Fig. 12). BCNU-induced accumulation of GSSG led to more severe Ca^{2+}-dependent damage compared to BSO-induced depletion of total glutathione (Fig. 9). Genetic knockdown and pharmacological inhibition of TRPC5 channel attenuated BCNU-induced cell death. From MTT assay, FACS analysis, and FRET-based Ca^{2+} measurement, I identified that Q111 cells have more sensitive to apoptotic cell death and intracellular Ca^{2+} change by BCNU than Q7. Mouse model of Huntington's disease (HD) is acutely vulnerable to redox state due to a loss of peroxiredoxin 1 (Prx1) in Q111 (59). Under reduced antioxidant activity in mutant Htt knock-in Q111 cells, Ca^{2+}-dependent toxicity can be mediated by TRPC5 channel.

Based on the TRPC1 channel is able to form receptor-operated heterotetrameric channel complexes with other TRPC channel subunits (29), TRPC1/C5 heteromultimer channel with voltage dependence similar to NMDA receptor channels significantly decreased calcium permeation, suggesting that TRPC1 contributes to the channel pore (60,61). Western blotting

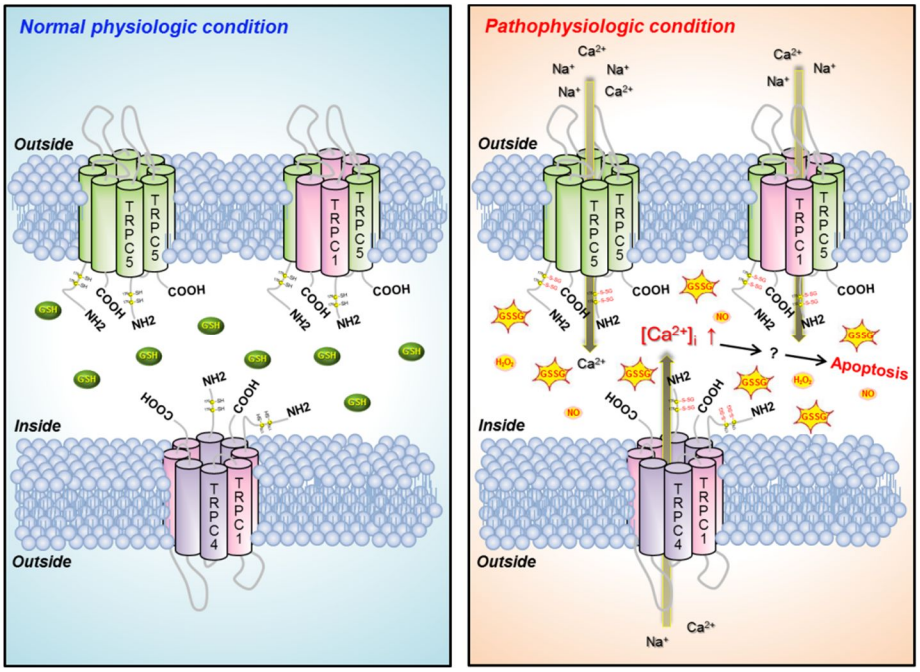

Fig. 12 Schematic model of TRPC5 S-glutathionylation for Huntington's disease

and mRNA analysis revealed expression of TRPC1 in Q111 at lower levels than Q7, but quantitative RT-PCR showed that TRPC1 proteins were expressed at similar levels in HD patient, (data not shown). TRPC1 channel has previously reported to be responsible for intracellular Ca^{2+}-dependent embryonic development (29) such as neuronal growth cones guidance (62) and neural stem cell proliferation (63). TRPC1 is downregulated in adult brain in respect with embryonic brain (29) as well as in vascular smooth muscle of aging model (64). In spite of genetic disorder, physical symptoms of HD typically become noticeable in mid-adult life and usually begin at a later age. Under glutathione homeostasis perturbations, decreased TRPC1 levels with aging are more likely to cause Ca^{2+} signaling failure, resulting in several age-related neurodegenerative disorders of the CNS including HD.

Although the physiological level of oxidative stress is indispensable and endurable, it can make nerve damage when defense and coping mechanisms against oxidative stress are impaired and altered. In BSO-induced depletion of total glutathione, both Q7 and Q111 were affected by low concentration of hydrogen peroxide (H_2O_2) (Fig. 9G and 10F,G).

In addition, BCNU increased FRET efficiency of YC6.1 in both cells, resulting from increases in intracellular calcium (Ca^{2+}). Highly sustained Ca^{2+} level in cytosol may lead to cell death due to disturbance of calcium homeostasis.

Likewise, elevated calcium level can induce calcium-dependent proteolysis. Proteolytic cleavage of huntingtin (Htt) is known to be a key event in the pathogenesis of Huntington's disease (HD) (65,66,67). Currently, proteolytic cleavage pathways have been reported for Htt *in vivo* that may influence cellular toxicity and aggregation by caspases (68), calpains (69,70), calcium/calmodulin-dependent protein kinase (71), and an unknown aspartic endopeptidase (72). Although this study does not show the relative contribution of calpain, caspases, or other proteases to HD progression, it suggests that BCNU-induced intracellular GSSG may trigger HD striatal cell death resulting from elevated calcium levels in cytosol.

The GSSG reductase inhibitor BCNU, clinically known as carmustine, is a proven chemotherapeutic agent (73). BCNU-dependent arrest of GSSG reductase activity leads to elevation of cellular GSSG and has chemotherapeutic functions. Based on findings from this study, physicians need to take a more cautious approach to prescribing BCNU agent for killing tumor

cells and minimizing oxidative stress related tissue injury.

In summary, I clarified the role of TRPC5 in Huntington's disease, showing the neuronal apoptosis caused by abnormal cytosolic Ca^{2+} through TRPC5, and demonstrated the activation mechanism in which cytosolic GSSG oxidizes to protein S-glutationylation (PSSG) in TRPC5. Although clinical symptoms of each disease are different from cell types and metabolic rate on the disease type, increased oxidative damage is a commonly described as a neuropathological feature, and is often accompanied by dysregulation of antioxidant scavenging systems (74). Elevated GSSG or newly produced ROS mediates and maintains intracellular oxidizing state since the impaired cellular GSH pool reduces resistance of cells toward radiation, anti-tumor or oxidative agent. These glutathione-dependent disorders may lead to not only neurodegenerative disorders but also aging, autoimmune diseases, and cancer in the cell types where TRPCs were expressed like in skeletal or smooth muscle (75), and kidney (76). No cells that express TRPC channels are free from impaired glutathione pool. Therefore, I expect that the findings from this study provide a better understanding on the role of TRPC channels in glutathione-related diseases.

REFERENCES

1. Bredesen, D.E., Rao, R.V., and Mehlen, P. (2006). Cell death in the nervous system. Nature *443*, 796–802.
2. Floyd, R.A. (1999). Antioxidants, oxidative, and degenerative neurological disorders. Proc. Soc. Exp. Biol. Med. *222*, 236–245.
3. Meister, A., and Anderson, M. (1983). Glutathione. Annu. Rev. Biochem. *52*, 711–760.
4. Cooper, A.J., Pinto, J.T., and Callery, P.S. (2011). Reversible and irreversible protein glutathionylation by respiratory substrates. Expert Opin. Drug Metab. Toxicol. *7*,891–910.
5. Hurd, T.R., Costa, N.J., Dahm, C.C., Beer, S.M., Brown, S.E., Filipovska, A., and Murphy, M.P. (2005). Glutathionylation of mitochondrial proteins. Antioxid. Redox Signal *7*, 999–1010.
6. Dalle–Donne, I., Colombo, G., Gagliano, N., Colombo, R., Giustarini, D., Rossi, R., and Milzani, A. (2011). S–glutathionylation in life and death decisions of the cell. Free Radic. Res. *45*, 3–15.
7. Townsend, D.M. (2007). S–glutathionylation: indicator of cell stress and regulator of the unfolded protein response. Mol. Interv. *7*, 313–324.
8. Lipton, S.A., Choi, Y.B., Takahashi, H., Zhang, D., Li, W., Godzik, A., and Bankston, L.A. (2002). Cysteine regulation of protein function–as exemplified by NMDA–receptor modulation. Trends Neurosci. *25*, 474–480.

9. Aracena-Parks, P., Goonasekera, S.A., Gilman, C., Dirksen, R.T., Hidalgo, C., and Hamilton, S.L., (2006). Identification of cysteines involved in S-nitrosylation, S-glutathionylation, and oxidation to disulfides in RyR1. J. Biol. Chem. *281*, 40354-40368.
10. Macpherson, L.J., Dubin, A.E., Evans, M.J., Marr, F., Schultz, P.G., Cravatt, B.F., and Patapoutian, A. (2007). Noxious compounds activate TRPA1 ion channels through covalent modification of cysteines. Nature *445*, 541-545.
11. Kashio, M., Sokabe, T., Shintaku, K., Uematsu, T., Fukuta, N., Kobayashi, N., Mori, Y., and Tominga, M. (2012). Redox signal-mediated sensitization of transient receptor potential melastin 2 (TRPM2) to temperature affects macrophage functions. Proc. Natl. Acad. Sci. USA *109*, 6745-6750.
12. Greka, A., Navarro, B., Oancea, E., Duggan, A., and Clapham, D.E. (2003). TRPC5 is a regulator of hippocampal neurite length and growth cone morphology. Nat. Neurosci. *6*, 837-845.
13. Plant, T.D., and Schaefer, M. (2003). TRPC4 and TRPC5: receptor-operated Ca^{2+}-permeable nonselective cation channels. Cell Calcium *33*, 441-450.
14. Yoshida, T., Inoue, R., Morii, T., Takahashi, N., Yamamoto, S., Hara, Y., Sato., Y., and Mori, Y. (2006). Nitric oxide activates TRP channels by cysteine S-nitrosylation. Nat. Chem. Biol. *2*, 596-607.
15. Xu, S., Sukumar, P., Zeng, F., Li, J., Jairaman, A., English, A., Naylor, J., Ciurtin, C., Sivaprasadarao, A., and Beech, D.J., et al. (2008). TRPC channel activation by extracellular thioredoxin. Nature *451*, 69-73.

16. Wong, C., Sukumar, P., Beech, D.J., and Yao, X., (2010). Nitric oxide lacks direct effect on TRPC5 channels but suppresses endogenous TRPC5-containing channels in endothelial cells. Pflugers Arch. *460*, 121-130.
17. Sian,J., Dexter, D.T., Lees, A.J., Daniel, S., Agid, Y., Javoy-Agid, F., Jenner, P., and Marsden, C.D. (1994). Alterations in glutathione levels in Parkinson's disease and other neurodegenerative disorders affecting basal ganglia. Ann. Neurol. *36*, 348-355.
18. Jeon, G.S., Kim, K.Y., Hwang, Y.J., Jung, M., An, S., Ouchi, M., Ouchi, T., Kowall, N., Lee, J., and Ryu H. (2012). Deregulation of BRCA1 leads to impaired spatiotemporal dynamics of γ-H2AX and DNA damage responses in Huntington's disease. Mol. Neurobiol. *45*, 550-563.
19. Erickson, M.G., Alseikhan, B.Z., Peterson, B.Z., and Yue, D.T. (2001). Preassociation of calmodulin with voltage-gated Ca(2+) channels revealed by FRET in single living cells. Neuron *31*, 973-985.
20. Truong, K., Sawano, A., Mizuno, H., Hama, H., Tong, K.I., Mal, T.K., Miyawaki, A., and Ikura, M. (2001). FRET-based by a new calmodulin-GFP fusion molecule. Nat. Struct. Biol. *8*, 1069-1073.
21. Vazquez, G., Wedel, B.J., Aziz, O., Trebak, M., and Putney, J.W.Jr, (2004). The mammalian TRPC cation channels. Biochim. Biophys. Acta. *1742*, 21-36.
22. Kang, T.M., Kim, Y.C., Sim, J.H., Rhee, J.C., Kim, S.J., Uhm, D.Y., So, I., and Kim, K.W. (2001). The properties of carbachol-activated nonselective cation channels at the

single channel level in guinea pig gastric myocytes. Jpn. J. Pharmacol. *85*, 291-298.

23. Gilmore, W.J., and Kirby, G.M. (2004). Endoplasmic reticulum stress due to altered cellular redox status positively regulates murine hepatic CYP2A5 expression. J. Pharmacol. Exp. Ther. *308*, 600-608.
24. Blair, N.T., Kaczmarek, J.S., and Clapham, D.E. (2009). Intracellular calcium strongly potentiates agonist-activated TRPC5 channels. J. Gen. Physiol. *133*, 525-546.
25. Pallardo, F., Markovic, E., and Vina, J. (2009). Cellular compartmentalization of glutathione. Masella, R., Mazza, G., (Eds), Glutathione and sulfur amino acids in human health and disease (Wiley & Sons, Inc., Hoboker New Jersey), 35-45.
26. Molleman, A. (2003). Patch clamping (John Wiley & Sons Ltd.).
27. Dalle-Donne, I., Milzani, A., Gagliano, N., Colombo, R., Giustarini, D., and Rossi, R. (2008). Molecular mechanisms and potential clinical significance of S-glutathionylation. Antioxid. Redox Signal. *10*, 445-473
28. Morgan, B., Ezerina, D., Amoako, T.N.E, Riemer, J, and Dick, T.P. (2012). Multiple glutathione disulfide removal pathways mediate cytosolic redox homeostasis. Nat. Chem. Biol. *9*, 119-125.
29. Strubing, C., Krapivinsky, G., K rapivinsky, L., and Clapham, D.E. (2003). Formation of novel TRPC channels by complex subunit interactions in embryonic brain. J. Biol. Chem. *278*, 39014-39019.

30. Kaneko, S., Kawakami, S., Hara, Y., Wakamori, M., Itoh, E., Minami, T., Takada. Y., Kume, T., Katsuki, H., Mori, Y., and Akike A. (2006). A critical role of TRPM2 in neuronal cell death by hydrogen peroxide. J. Pharmacol. Sci. *101*, 66-76.
31. Ascenzi, P., Colasanti, M., Persichini, T., Muolo, M., Polticelli, F., Venturini, G., Bordo, D., and Bolognesi, M. (2000). Re-evaluation of amino acid sequence and structural consensus rules for cysteine-nitric oxide reactivity. Biol. Chem. *381*, 623-627.
32. Rhee S.G., Bae Y.S., Lee, S.R., Kwon, j. (2000). Hydrogen peroxide: a key messenger that modulates protein phosphorylation through cysteine oxidation. Sci. STKE. 2000(53).
33. Jung, S., Muhle, M., Schaefer, M., Strotmann, R., Schultz, G., and Plant, T.D. (2003). Lanthanides potentiate TRPC5 currents by an action at extracellular sites close to the pore mouth. J. Biol. Chem. *278*, 3562-3571.
34. Lee, Y.M., Kim, B.J., Yang, D.K., Zhu, M.H., Lee, K.P., So, I., and Kim, K.W. (2003). TRPC5 as a candidate for nonselective cation channel activated by muscarinic stimulation in murine stomach. Am. J. Physiol. *284*, 604-616.
35. Kanki, H., Kinoshita, M., Akaike, A., Satoh, M., Mori, Y., and Kaneko, S. (2001). Activation of inositol 1,4,5-trisphosphate receptor is essential for opening of mouse TRP5 channels. Mol. Pharmacol. *60*, 989-998.
36. Fowler, M.A., Sidiropoulou, K., Ozkan, E.D., Phillips, C.W., and Cooper, D.C. (2007). Corticolimbic expression of

TRPC4 and TRPC5 channels in the rodent brain. PLos One. *27*, e573.

37. Rao, A.V., and Balachandran, B. (2002). Role of oxidative stress and antioxidants in neurodegenerative diseases. (Maney Publishing).
38. Zhang, C., Roepke, T.A., Kelly, M.J., and Ronnekleiv, O.K. (2008). Kisspeptin depolarizes Gonadotropin-releasing hormone neurons through activation of TRPC-like cationic channels. J. Neurosci. *23*, 4423-4434.
39. Miller, M., Shi, J., Zhu, Y., Kustov, M., Tian, J.B., Stevens, A., Wu, M., and Zhu, M.X. (2011). Identification of ML204, a novel potent antagonist that selectively modulates native TRPC4/C5 ion channels. J Biol. Chem. *286*, 33436-33446.
40. Lee, M., Cho, T., Jantaratnotai, N., Wang, Y.T., McGeer, E., and McGeer, PL. (2010). Depletion of GSH in glial cells induces neurotoxicity: relevance to aging and degenerative neurological diseases. FASEB J. *24*, 2533-2545.
41. Dalle-Donne, I., Rossi, R., Colombo, G., Giustarini, D., Milzani, A. (2009). Protein S-glutathionylation: a regulatory device from bacteria to humans. Trends Biochem. Sci. *34*, 85-96.
42. Mieyal, J.J., Gallogly, M.M., Qanungo, S., Sabens, E.A., Shelton, M.D. (2008). Molecular mechanisms and clinical implications of reversible protein S-glutathionylation. Antioxid. Redox Signal. *10*, 1941-1988.
43. Park, H.A., Khanna, S., Rink, C., Gnyawali, S, Roy, S., Sen, C.K. (2009). Glutathione disulfide induces neural cell death via a 12-lipoxygenase pathway. Cell Death Differ. *16*, 1167-1179.

44. Dalle-Donne, I., Rossi, R., Giustarini, D., Colombo, R., Milzani, A. (2007). S-glutathionylation in protein redox regulation. Free Radic. Biol. Med. *43*, 883-898.
45. Cho, H.C., Tsushima, R.G., Nquyen, T.T., Guy, H.R., Backx, P.H. (2000). Two critical cysteine residues implicated in disulfide bond formation and proper folding of Kir2.1. Biochemistry *39*, 4649-4657.
46. Leyland, M.L., Dart, C., Spencer, P.J., Sutcliffe, M.J., Stanfield P.R. (1999). The possible role of a disulphide bond in forming functional Kir2.1 potassium channels. Pflugers Arch. *438*, 778-781.
47. Yang, Y., Shi, W., Chen, X., Cui, N., Konduru, A.S., Shi, Y., Trower, T.C., Zhang, S., Jiang, C. (2011). Molecular basis and structural insight of vascular K(ATP) channel gating by S-glutathionylation. J. Biol. Chem. *286*, 9298-9307.
48. Zeron, M.M., Chen, N., Moshaver, A., Lee, A.T., Wellington, C.L., Raymond, L.A. (2001). Mutant huntingtin enhances excitotoxic cell death. Mol. Cell Neurosci. *17*, 41-53.
49. Seto-Ohshima, A., Emson, P.C., Lawson, E., Mountjoy, C.Q., Carrasco, L.H. (1988). Loss of matrix calcium-binding protein-containing neurons in Huntington's disease. Lancet 1252-1255.
50. Zeron, M.M., Hansson, O., Chen, N., Wellington, C.L., Leavitt, B.R., Raymond, L.A. (2002). Increased sensitivity to N-methyl-D-aspartate receptor-mediated excitotoxicity in a mouse model of Huntington's disease. Neuron *33*, 849-860.
51. Chen, N., Luo, T., Wellington, C., Metzler, M., McCutcheon, K., Raymond, L.A. (1999). Subtype-specific enhancement

of NMDA receptor currents by mutant huntingtin. J. Neurochem. *72*, 1890-1898.

52. Sun, Y., Savanenin, A., Reddy, P.H., Liu, Y.F. (2001). Polyglutamine-expanded huntingtin promotes sensitization of N-methyl-D-aspartate receptors via post-synaptic density 95. J. Biol. Chem. *276*, 24713-24718.
53. Tang, T.S., Tu, H., Chan, E.Y., Maximov, A., Wang, Z., Wellington, C.L., Bezprozvanny, I. (2003). Huntingtin and huntingtin-associated protein 1 influence neuronal calcium signaling mediated by inositol-(1,4,5) triphosphate receptor type 1. Neuron *39*, 227-239.
54. Choo, Y.S., Johnson, G.V., MacDonald, M., Detloff, P.J., Lesort, M. (2004). Mutant huntingtin directly increases susceptibility of mitochondria to the calcium-induced permeability transition and cytochrome c release. Hum. Mol. Genet. *13*, 1407-1420.
55. Lin, M.T., and Beal, M.F. (2006). Mitochondrial dysfunction and oxidative stress in neurodegenerative diseases. Nature *443*, 787-795.
56. Pias, E.K., and Aw, T.Y. (2002). Apoptosis in mitotic competent undifferentiated cells is induced by cellular redox imbalance independent of reactive oxygen species production. FASEB J. *16*, 781-790.
57. Coyle, J.T., Puttfarcken, P. (1993). Oxidative stress, glutamate, and neurodegenerative disorders. Science *262*, 689-695.
58. Herrera, F., Martin, V., Garcia-Santos, G., Rodriguez-Blanco, J., Antolin, I, Rodriguez, C. (2007). Melatonin

prevents glutamate-induced oxytosis in the HT22 mouse hippocampal cell line through an antioxidant effect specifically targeting mitochondria. J. Neurochem. *100*, 736-746.

59. Pitts, A., Dailey, K., Newington, J.T., Chien, A., Arseneault, R., Cann, T., Thompson, L.M., and Cumming, R.C. (2012). Dithiol-based compounds maintain expression of antioxidant protein peroxiredoxin 1 that counteracts toxicity of mutant huntingtin. J. Biol. Chem. *287*, 22717-22729.
60. Strubing, C., Krapivinsky, G., Krapivinsky, L., Clapham, D.E. (2001). TRPC1 and TRPC5 form a novel cation channel in mammalian brain. Neuron *29*, 645-655.
61. Storch, U., Forst, A.L., Philipp, M., Gudermann, T., Mederos Schnitzler, M. (2012). Transient receptor potential channel 1 (TRPC1) reduces calcium permeability in heteromeric channel complexes. J. Biol. Chem. *287*, 3530-3540.
62. Shim, S., Goh, E.L., Ge, S., Salior, K., Yuan, J.P., Roderick, H.L., Bootman, M.D., Worley, P.F., Song, H., Ming, G.L. (2005). XTRPC1-dependent chemotropic guidance of neuronal growth cones. Nat. Neurosci. *8*, 730-735.
63. Fiorio Pla, A., Maric, D., Brazer, S.C., Giacobini, P., Liu, X., Chang, Y.H., Ambudkar, I.S., Barker, J.L. (2005). Canonical transient receptor potential 1 plays a role in basic fibroblast growth factor (bFGF)/FGF receptor-1-induced Ca2+ entry and embryonic rat neural stem cell proliferation. J. Neurosci. *25*, 2687-2701.
64. Erac, Y., Selli, C., Kosova, B., Akcali, K.C., Tosun, M. (2010). Expression levels of TRPC1 and TRPC6 ion

channels are reciprocally altered in aging rat aorta: implications for age-related vasospastic disorders. Age (Dordr). *32*, 223-230.

65. Miller, J.P., Holcomb, J., AI-Ramahi, I., de Haro, M.,Gafni, J., Ellerby, L.M., et al. (2010). Matrix metalloproteinases are modifiers of huntingtin proteolysis and toxicity in Huntington's disease. Neuron *67*(2), 199-212.
66. Mattson, M.P. (2007). Calcium and neurodegeneration. Aging Cell *6*, 337-350.
67. Marambaud, P., Dreses-Werringloer, U., Vingdeux, V. (2009). Calcium signaling in neurodegeneration. Mol. Neurodegener. *4*:20.
68. Wellington, C.L., Singaraja, R., Elleby, L., Savill, J., Roy, S., Leavitt, B., Cattaneo, E., Bredesen, D.E., Hayden, M.R. (2000). Inhibiting caspase cleavage of huntingtin reduces toxicity and aggregate formation in neuronal and nonneuronal cells. J. Biol. Chem. *275*, 19831-19838.
69. Kim, Y.J., Yi, Y., Sapp, E., Wang, Y., Cuiffo, B., Kegel, K.B., Qin, Z.H., Aronin, N., DiFiglia, M. (2001). Caspase 3-cleaved N-terminal fragments of wild type and mutant huntingtin are present in normal and Huntington's disease brains, associate with membranes, and undergo calpain-dependent proteolysis. Proc. Natl. Acad. Sci. U.S.A. *98*, 12784-12789.
70. Gafni, J., Hermel, E., Young, J.E., Wellington, C.L. Hayden, M.R., Ellerby, L.M. (2004). Inhibition of calpain cleavage of huntingtin reduces toxicity: accumulation of calpain/caspase fragments in the nucleus. J. Biol. Chem. *279*, 20211-20220.

71. McGinnis, K.M., Whitton, M.M., Gnegy, M.E., Wang K.K. (1998). Calcium/calmodulin-dependent protein kinase IV is cleaved by caspase-3 and calpain in SH-SY5Y human neuroblastoma cells undergoing apoptosis. J. Biol. Chem. *273*, 19993-20000.
72. Lunkes, A., Lindenberg, K.S., Ben-Haiem, L., Weber, C., Devys, D., Landwehrmeyer, G.B., Mandel, J.L., Trottier, Y. (2002). Proteases acting on mutant huntingtin generate cleaved products that differentially build up cytoplasmic and nuclear inclusions. Mol. Cell *10*, 259-269.
73. Chang, S.M., Prados, M.D., Yung, W.K., Fine, H., Junck, L., Greenberg, H., Robins, H.I., Mehta, M., Fink, K.L., Schold, C. (2004). Phase II study of neoadjuvant 1, 3-bis (2-chloroethyl)-1-nitrosourea and temozolomide for newly diagnosed anaplastic glioma: a North American Brain Tumor Consortium Trial. Cancer *100*, 1712-1716.
74. Sabens Liedhegner, E.A., Gao, X., Mieyal, J.J. (2012). Mechanism of altered redox regulation in neurodegenerative diseases-focus on S-glutathionylation. Antioxid. Redox Signal. *16*, 543-566.
75. Jenner, A.M., Ruiz, J.E., Dunster, C., Halliwell, B., Mann, G.E., and Siow, R.C. (2002). Vitamin C protects against hypochlorous acid-induced glutathione depletion and DNA base and protein damage in human vascular smooth muscle cells. Arterioscler. Thromb. Vasc. Biol. *22*, 574-580.
76. Brezis, M., Rosen, S., Silva, P., and Epstein, F.H. (1983). Selective glutathione depletion on function and structure of the isolated perfused rat kidney. Kidney Int. *24*, 178-184.

국문 초록

서론 : 정상 칼슘신호는 신경의 생리학적 기능에 중요하지만, 비정상적인 칼슘농도는 신경퇴행성질환의 병리학적 질병의 원인이 된다. 최근 칼슘투과성과 비선택적 양이온통로인 TRP 이온통로가 특정한 상태에서 산화과정을 통해 세포 내 칼슘항상성에 문제를 야기할 수 있는 것으로 알려졌다. 그러나 이런 예기치 않은 산화와 그 활성기전에 대한 이해는 현재까지도 연구가 진행 중이며, 여전히 정확한 분자적 접근이 미비한 상태이다.

결과 : 이 연구에서 일부 산화제, DTNP (125 ± 25 pA/pF, n=6), DTNB (12 ± 3 pA/pF, n=6), 2-PDS (122 ± 58 pA/pF, n=6) and H_2O_2 (47 ± 19 pA/pF, n=6)가 TRPC4와 TRPC5 이온통로를 활성화하는 것을 전세포 전류기록을 통해서 확인했다. 세포 내 산화된 글루타치온 역시 TRPC1, TRPC4와 TRPC5 이온통로의 활성을 조절하는 것으로 밝혔다. 이런 활성은 TRPC 이온통로의 세포질에 높게 보존된 시스테인 아미노산들 중 TRPC5 단백질의 176번째와 178번째 시스테인 두 곳에 직접 결합하는 것을 단백질 상호면역침강을 통해 확인했다. 헌팅턴 유전자를 삽입한 쥐의 선조체 세포주에서 TRPC4와 TRPC5의 발현을 관찰하였다. 그리고 carmustine (BCNU)과 L-buthionine (S,R) sulfoximine (BSO)으로 세포 내 글루타치온의 농도를 변화시켜서, 세포 내 산화된 형태의 글루타치온의 양을 증가시켰더니 헌팅턴 세포주에서 세포괴사가 유도되는 것을 알 수 있었다. BSO를 전처리하여 세포 내 글루타치온을 고갈시키고 난 뒤, 과산화수소에 대한 세포괴사가 더 낮은 농도에서 민감하게 나타났다. FRET 기반으로 한 칼슘측정을 통해 BCNU에 의해 세포 내 칼슘상태가 높게 유지되는 것을 알아냈다. 이런 칼슘 의존적 세포괴사와 TRPC5의 연관성을 확인하기 위해 RNA 방해기술인 TRPC5 siRNA를 발현하거나 TRPC 이온통로의 저해제인 카드뮴 또는 ML204를 사용하면, BCNU에 의해 유도된 세포괴사가 감소하는 것을 유세포분석과 MTT 분석을 통해 확인하였다.

결론 : 이 결과를 통해 세포 내 산화된 형태의 글루타치온이 TRPC5를 직접 산화함으로써 이온통로의 활성을 유도하여 세포 내 칼슘증가를 초래하고, 이 칼슘의 비정상적인 신호전달로 인하여 헌팅턴병의 원인이 될 것으로 생각한다. 그러므로 지금까지 알려진 신경퇴행성질환이 TRPC5 이온통로의 산화가 새로운 원인인자가 될 수 있다는 결론을 도출하였다.

주요어 : TRPC5, 산화과정, 글루타치온, 헌팅턴병

학 번 : 2009-21910